© 2016. Published by The Company of Biologists Ltd | Development (2016) 143, 2066-2076 doi:10.1242/dev.131292

STEM CELLS AND REGENERATION

RESEARCH ARTICLE

Ihha induces hybrid cartilage-bone cells during zebrafish jawbone regeneration

Sandeep Paul*, Simone Schindler*, Dion Giovannone, Alexandra de Millo Terrazzani, Francesca V. Mariani and J. Gage Crump‡

ABSTRACT

The healing of bone often involves a cartilage intermediate, yet how such cartilage is induced and utilized during repair is not fully understood. By studying a model of large-scale bone regeneration in the lower jaw of adult zebrafish, we show that chondrocytes are crucial for generating thick bone during repair. During jawbone regeneration, we find that chondrocytes co-express genes associated with osteoblast differentiation and produce extensive mineralization, which is in marked contrast to the behavior of chondrocytes during facial skeletal development. We also identify the likely source of repair chondrocytes as a population of Runx2^{+}/Sp7^{-} cells that emanate from the periosteum, a tissue that normally contributes only osteoblasts during homeostasis. Analysis of *Indian hedgehog homolog a* (*ihha*) mutants shows that the ability of periosteal cells to generate cartilage in response to injury depends on a repair-specific role of Ihha in the induction as opposed to the proliferation of chondrocytes. The large-scale regeneration of the zebrafish jawbone thus employs a cartilage differentiation program distinct from that seen during development, with the bone-forming potential of repair chondrocytes potentially due to their derivation from osteogenic cells in the periosteum.

KEY WORDS: Bone regeneration, Zebrafish, Jaw, Chondrocyte, Osteoblast, Ihha, Chondroid bone

INTRODUCTION

Although large bone lesions often fail to repair in mammals, many reptiles, amphibians and fishes can regenerate entire appendicular, tail and jaw skeletons (Goss and Stagg, 1958; Graver, 1978; Ghosh et al., 1994; Brockes, 1997; Iovine, 2007). A commonality between large-scale bone regeneration in these species and fracture healing in humans is the formation of a cartilage callus that bridges the wound, in particular when the fracture is not mechanically stabilized (Pritchard and Ruzicka, 1950; Lieberman and Friedlaender, 2005). Current models of bone regeneration in zebrafish focus on the fin and calvaria, yet in these models bone regenerates through de-differentiation of existing osteoblasts (Knopf et al., 2011; Geurtzen et al., 2014), or alternatively, *de novo* generation of osteoblasts (Singh et al., 2012). By contrast, we show here that regeneration of the zebrafish lower jawbone involves a prominent cartilage intermediate, which has allowed us to better understand the nature and requirement of cartilage in large-scale bone regeneration.

Department of Stem Cell Biology and Regenerative Medicine, Keck School of Medicine, University of Southern California, Los Angeles, CA 90033, USA.
*These authors contributed equally to this work

‡Author for correspondence (gcrump@usc.edu)

J.G.C., 0000-0002-3209-0026

Received 24 September 2015; Accepted 12 April 2016

During mammalian endochondral bone development, *Sox9*$^{+}$ mesenchymal cells condense to form chondrocytes, which produce extracellular matrix proteins such as type II collagen (encoded by *Col2a1*) and later, hypertrophy-associated factors such as type X collagen (*Col10a1*) and connective tissue growth factor (*Ctgf*) (Mackie et al., 2008). Whereas many hypertrophic chondrocytes undergo apoptosis, it has been suggested that some chondrocytes escape apoptosis and generate long-lived osteocytes (Mayne et al., 1976; von der Mark and von der Mark, 1977; Yang et al., 2014; Zhou et al., 2014). In the hypertrophic zone, blood vessels invade the zone of dying chondrocytes and bring along osteoprogenitors derived from the periochondrium and periosteum (Maes et al., 2010). Osteoblast precursors initially express high levels of *Runx2*, and then *Sp7* (*Osterix*) and type I collagen (*Col1a1*) as they differentiate into early osteoblasts (Ortuno et al., 2013). As osteoblasts further mature, they express genes associated with mineralization, including *Spp1* (*Osteopontin*) and *Bglap* (*Osteocalcin*). However, hypertrophic chondrocytes also express low levels of many of these osteoblast genes (with the possible exception of *Bglap*) and produce a mineralized (i.e. calcified) matrix (Dy et al., 2012). During mammalian fracture repair, cells within the cartilage callus have been shown to produce BGLAP and contain dense collagen fibers typical of bone, suggesting that these repair chondrocytes have bone-like properties (Bahney et al., 2014). By comparing bone generation during development with bone regeneration in the adult zebrafish jaw, we find that developmental and regenerating chondrocytes differ in the timing and extent of osteoblast-associated gene expression, as well as their capacity for mineralization.

Bones, including those in fish, are dynamic organs that undergo remodeling in response to biomechanical forces, with osteoclasts removing old bone and osteoblasts adding new bone (Apschner et al., 2011). The source of new osteoblasts during bone homeostasis is the periosteum, a layer of connective tissue surrounding bone (Ono et al., 2014). In mammalian bone fractures, the periosteum also appears to contribute first to cartilage and then to bone during repair (Murao et al., 2013). An important question then is how the periosteum, which makes only bone during homeostasis, then also makes cartilage during repair. A previous study had shown that BMP2 is sufficient to promote the chondrogenic differentiation of the periosteum in mice (Yu et al., 2010). Here, we show a novel requirement for Indian Hedgehog (Ihh) signaling in the differentiation of periosteal cells into chondrocytes during zebrafish jawbone regeneration.

In mammals, Hh signaling is known to have multiple roles in regulating the development of growth plate chondrocytes and osteoblasts. Ihh is produced by hypertrophic chondrocytes, where it signals to neighboring pre-hypertrophic chondrocytes to promote their proliferation (St-Jacques et al., 1999; Long et al., 2001). Ihh also acts on periochondral cells to induce osteoblast differentiation,

Development (2016) 143, 2066-2076 doi:10.1242/dev.131292

with deletion of the Ihh co-receptor *Smo* in the perichondral lineage leading to loss of endochondral bone (Long et al., 2004). Notably, hypertrophic chondrocytes themselves appear to be unresponsive to Ihh, which may explain the lack of high levels of osteoblast genes (e.g. *Runx2*, *Col1a1*, *Spp1*, *Bglap*) in growth plate chondrocytes (Long et al., 2001). However, elevation of Hh signaling in zebrafish, either by loss of the negative regulators *ptc1* and *ptc2* or treatment with the Hh pathway agonist purmorphamine, can induce osteoblast gene expression in chondrocytes, suggesting plasticity in the ability of developmental chondrocytes to express osteoblast-associated genes (Hammond and Schulte-Merker, 2009). In mice, stimulation of the Hh pathway can also promote the formation of bone in several skeletal injury contexts, although the mechanism by which Hh does so is not well understood (Baht et al., 2014; Huang et al., 2014; Zou et al., 2014). Specifically, none of these studies examined whether the increase in bone production is due to an effect on osteoprogenitor differentiation, an effect on chondrocytes, or both. By analyzing an adult viable *Indian hedgehog homolog a* (*ihha*) mutant in zebrafish, we find an unexpected role for Ihha in inducing the differentiation of periosteal cells into bone-producing chondrocytes during jawbone regeneration.

RESULTS

The lower jawbone of adult zebrafish regenerates through a cartilage intermediate

Previous reports have shown that, despite their development as directly differentiating intramembranous bones, the jawbones of newts regenerate through a cartilage intermediate (Graver, 1978; Ghosh et al., 1994). We therefore tested whether a similar process occurs in zebrafish. Using spring scissors, we removed approximately half (1.6-1.8 mm) of the lower jawbone on one side of the adult zebrafish, from the insertion point of the maxillary barbell to just past and including the anterior end of Meckel's cartilage (Fig. 1A and Fig. S1). Analysis of regeneration revealed first cartilage and then bone filling in the lesion (Fig. 1B,C). Within 7 days post-resection (dpr), cartilage bridged the resected area in 6/9 animals, and by 14 dpr, numerous new fragments of Alizarin Red^{+} mineralized matrix were present in 11/11 animals. At 35 dpr, bone-like matrix fully spanned the lesion in 7/7 animals, with bone regaining the characteristic features of the lower jaw, e.g. the anguloarticular prominence, in three cases. Bone microcomputed tomography (μCT) confirmed extensive bone repair by 28 and 35 dpr (Fig. 1E and Movies 1 and 2). Although the distal-most tips of the zebrafish jaw have been reported to undergo epimorphic regeneration following amputation (Wang et al., 2012), we found it necessary to leave the skin to achieve successful regeneration of these larger resections (data not shown).

In order to understand jawbone regeneration at the tissue level, we performed Haematoxylin and Eosin (H&E) staining on sections (Fig. 1D). By 10 dpr, we observed chondrocytes within an extensive callus bridging the resected area, with some areas at the borders of the cartilage callus beginning to adopt an appearance reminiscent of bone. Of note, the initial induction of the cartilage callus occurs throughout the resected region, including near the anterior cut site in which Meckel's cartilage and its associated periochondrium had been completely removed (Fig. S1). Our findings are therefore in agreement with previous studies in amphibians showing that the remnant Meckel's cartilage and its perichondrium are not the main source of the cartilage callus during lower jawbone regeneration (Hall and Hanken, 1985). At 30 dpr, a substantial amount of new bone was observed in association with the cartilage callus, and by 60 dpr, the cartilage callus had largely disappeared and been replaced by large bone fragments separated by small gaps. The transient nature of the cartilage callus indicates that bone, but not Meckel's cartilage, regenerates following jaw resection in adult zebrafish, with jawbone regeneration being similar to mammalian

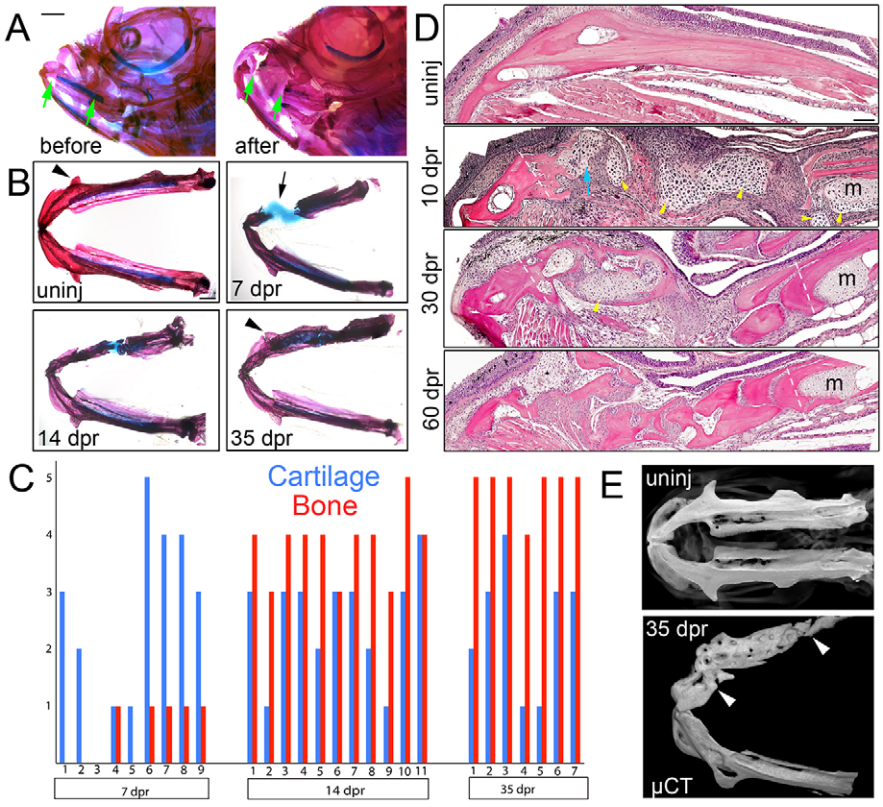

Fig. 1. Regeneration of the lower jawbone in adult zebrafish. (A) Whole-mount views of adult zebrafish heads before and after resection stained with Alizarin Red and Alcian Blue to label bone and cartilage. Arrows show resection sites. (B) Dissected lower jaws show the time course of cartilage and bone formation during regeneration. Arrow denotes the repair cartilage that has contracted somewhat during mounting. Arrowheads indicate regeneration of the anguloarticular prominence. (C) Qualitative assessment of cartilage and bone formation during lower jaw regeneration in individual animals. The *y*-axis shows the amount of cartilage/bone in the lesion from none (0) to full spanning (5). (D) H&E staining on sections of the lower jawbone before and after resection. An extensive cartilage callus (yellow arrowheads) is seen at 10 dpr, including at the anterior cut site (blue arrow) devoid of Meckel's cartilage (m). Dashed lines show resection sites. (E) Bone μCT images show ventral views of lower jawbones from uninjured (uninj) and regenerated animals. Arrowheads indicate resection sites. See also Movie 1. Scale bars: 1 mm in A,B and 100 μm in D.

Development (2016) 143, 2066-2076 doi:10.1242/dev.131292

fracture repair, involving a transient cartilage callus that is replaced by bone (Bahney et al., 2014).

Co-expression of genes associated with chondrocyte and osteoblast lineages in the regenerating cartilage callus

Given the observed conversion of cartilage to bone during jawbone repair, we next examined the expression of genes typically associated with chondrocytes and osteoblasts (Fig. 2A). As early as 6 dpr, we observed expression of *sox9a* and *col2a1a* in the nascent cartilage callus, with expression increasing by 8-10 dpr. Repair chondrocytes later expressed markers typical of hypertrophy, including *col10a1* by 8 dpr (Fig. 2A) and *ctgfa* at 14 dpr (Fig. S2C). Unexpectedly, we also observed expression of *runx2b* and *col1a1a* (genes normally associated with early osteoblasts) in chondrocyte-like cells as early as 6 dpr, with expression continuing through 8 and 10 dpr. Expression of *spp1* and *sp7* (genes associated with maturing osteoblasts) also became apparent in chondrocyte-like cells by 10 dpr (Fig. 2A and Fig. S2A,B). Multicolor fluorescent *in situ* hybridization confirmed that the same cells within the repaired jaw callus co-express *col2a1a* and either *col1a1a* or *runx2b* at 10 dpr (Fig. 2B), with many cells co-expressing *col1a1a*, *col2a1a* and *col10a1* by 14 dpr (Fig. S2E). Cells within the cartilage callus also produce Sox9, Col2a1, Col1a1 and Sp7 proteins (Fig. S3). Thus, cells within the cartilage callus not only express genes associated with cartilage differentiation and hypertrophy, but also dynamically express high levels of genes commonly associated with osteoblast differentiation (summarized in Fig. 2C).

Repair chondrocytes mineralize and express mature osteoblast markers

As we found that repair chondrocytes express many genes associated with osteoblast differentiation, we next examined their ability to produce mineralized matrix and express mature osteoblast markers. At 8 dpr, Trichrome staining revealed the production of dense collagen fibers around some repair chondrocytes, which were similar in appearance to the osteoid-like substance surrounding bones (Fig. 3A). Repair chondrocytes labeled by a *col2a1a*^{BAC}:GFP transgene began to produce Alizarin Red^{+} mineralized matrix by 12 dpr (data not shown), and by 30 dpr, *col2a1a*^{BAC}:GFP^{+} cells were embedded within a continuous sheet of Alizarin Red^{+} mineralized matrix (Fig. 3B). A comparison of adjacent sections stained for *col2a1a*^{BAC}:GFP and processed for H&E histology confirmed the presence of *col2a1a*^{BAC}:GFP-derived cells embedded in new bone (Fig. S4). Consistent with most mineralization occurring through a chondrocyte intermediate, the majority of cells expressing the osteoblast-associated gene *spp1* at 16 dpr were *col2a1a*^{BAC}:GFP^{+} (Fig. 3C). The long-lived nature of GFP protein (Fig. S5) further allowed us to perform short-term lineage tracing of

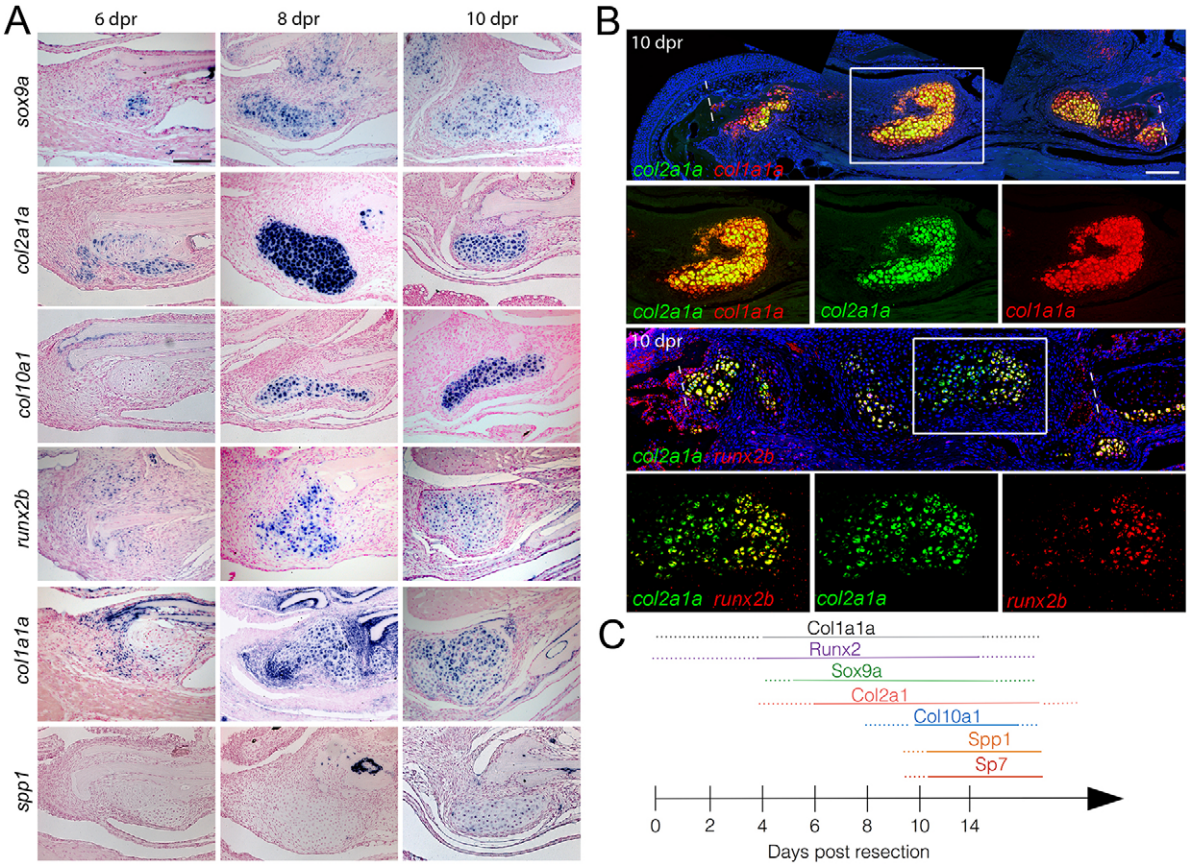

Fig. 2. Co-expression of chondrocyte and osteoblast genes in repair cartilage. (A) Colorimetric *in situ* hybridization shows gene expression in the cartilage callus anterior to the cut site of the lower jawbone. The chondrocyte markers *sox9a* and *col2a1a* are seen in the cartilage callus by 6 dpr, with a peak of expression at 8 dpr. Expression of the hypertrophic chondrocyte marker *col10a1* begins at 8 dpr. The osteoblast markers *runx2b* and *col1a1a* are expressed in mesenchyme and early cartilage at 6 dpr and beyond. By 10 dpr, expression of the osteoblast marker *spp1* is evident in the cartilage callus. (B) Two-color fluorescent *in situ* hybridization shows co-expression of *col2a1a* with *col1a1a* or *runx2b* at 10 dpr. Dashed lines show resection sites and magnified regions (white boxes) demonstrate that individual cells co-express both markers. Hoechst labels nuclei in blue. (C) Summary of the time course of expression within the cartilage callus. Scale bars: 100 µm.

Development (2016) 143, 2066-2076 doi:10.1242/dev.131292

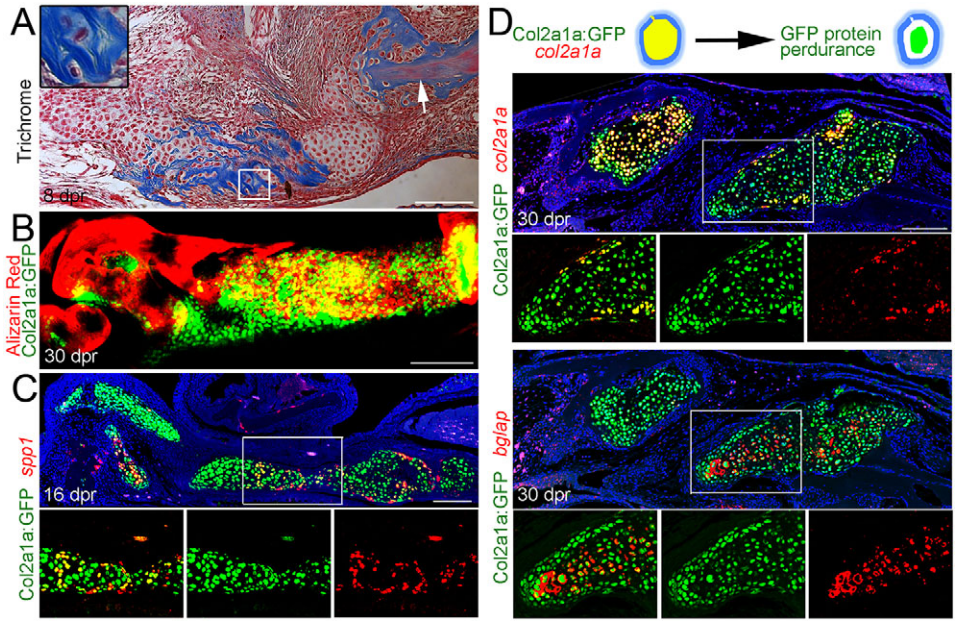

Fig. 3. Mineralization and osteoblastic maturation of repair chondrocytes. (A) Trichrome staining at 8 dpr reveals the presence of collagen-rich osteoid-like material surrounding individual chondrocytes of the regenerating jaw. Inset shows a magnified view of several chondrocytes. Note the similar appearance of collagen staining (blue) between the unresected jawbone (arrow) and the mineralizing cartilage. (B) Alizarin Red staining of the regenerating jawbone in live adult zebrafish shows mineralization of *col2a1a*^{BAC}:GFP-expressing chondrocytes. (C) Fluorescent *in situ* hybridization together with anti-GFP immunohistochemistry shows a subset of *col2a1a*^{BAC}:GFP^{+} chondrocytes co-expressing the osteoblast marker *spp1*. (D) Schematic showing that GFP protein perdures in cells long after endogenous *col2a1a* mRNA ceases to be produced. In the fluorescent *in situ* images of regenerating jawbone at 30 dpr, cells of the left callus still express *col2a1a* whereas cells of the right callus have largely ceased *col2a1a* expression and now express high levels of *bglap* (*osteocalcin*). Retention of GFP protein shows that *bglap*$^{+}$ cells arise from cells that previously expressed *col2a1a*^{BAC}:GFP. Areas in the white boxes are magnified and presented as merged and individual channels. Scale bars: 100 µm.

col2a1a^{BAC}:GFP-derived cells. At 30 dpr, many cells within the *col2a1a*^{BAC}:GFP^{+} callus retained GFP protein but no longer expressed *col2a1a*, with *col2a1a*$^{-}$ cells instead expressing the mature osteoblast marker *bglap* (*osteocalcin*) (Fig. 3D). These findings reveal that, as repair proceeds, chondrocytes shut down chondrocyte matrix genes, produce mineralized matrix and upregulate mature osteoblast genes.

Growth plates of developing zebrafish cartilages have largely distinct zones of chondrocyte and osteoblast gene expression

As the co-expression of chondrocyte and osteoblast genes during jawbone regeneration was unexpected, we examined in more detail how this compares with skeletal development in zebrafish. Although the lower jawbone regenerates through a cartilage intermediate, this bone develops through the direct differentiation of progenitors into osteoblasts (i.e. intramembranous ossification). We therefore examined the development of the ceratohyal, a bone that forms through a cartilage intermediate in the face, to understand how the cartilage template might differ between development and regeneration. At 28 days post-fertilization (dpf), triple labeling with an *sp7*:GFP transgene, *col10a1 in situ* hybridization and BrdU incorporation revealed a mammalian-like growth plate arrangement within the ceratohyal (Fig. 4B,C). At this stage, overlapping *col2a1a* and BrdU labeling marked a proliferative zone, *col10a1* a hypertrophic zone and *sp7*:GFP and *bglap* the periosteum. Distinct proliferative and hypertrophic zones were also observed in other cartilages, including the lower jaw Meckel's cartilage. Further analysis of the ceratohyal at 14 dpf revealed *sox9a* and *col2a1a* expression in a subset of chondrocytes at either end, *col1a1a* expression within the periosteum and a few chondrocytes at the hypertrophic border, and *spp1* solely within the periosteum (Fig. 4C). By 21 dpf, *col1a1a* became restricted to periosteal cells, with *col2a1a* continuing to label chondrocytes at both ends of the ceratohyal. At 16 dpf, Alizarin Red staining of *col2a1a*^{BAC}:GFP^{+} fish revealed mineralization around but not within the ceratohyal cartilage (Fig. 4D), correlating with expression of *col1a1a*, *spp1*, *bglap* and *sp7*:GFP in the periosteum. Even in 49 dpf juvenile fish, mineralization was observed only around the cartilage, with *col2a1a*^{BAC}:GFP continuing to label two growth plate-like zones of chondrocytes. Although the lower jaw Meckel's cartilage fails to mineralize and persists into adulthood in zebrafish, we observed a similar absence of *col1a1a* mRNA and *sp7*:GFP and *osteocalcin*:GFP transgenes in Meckel's chondrocytes at juvenile and adult stages (Fig. S2F-H). Thus, in contrast to the transient chondrocytes during adult jawbone repair, developmental chondrocytes in zebrafish do not express high levels of osteoblast genes such as *spp1*, *bglap* and *sp7*, and fail to mineralize. These molecular differences further support the transient repair callus being distinct from Meckel's cartilage.

Periosteal cells probably contribute to the cartilage callus during jawbone regeneration

As the periosteum has been suggested to contribute to the cartilage callus in mammalian fractures (Murao et al., 2013), we next investigated whether it also contributes to zebrafish jawbone regeneration. H&E staining revealed that, as with bones in other species, the adult lower jawbone is covered with a thin lining of connective tissue, the periosteum. At 2 dpr, we observed a marked expansion of the periosteum, which now extended to cover the cut ends of the bone (Fig. 5A,B). By 4 dpr, the number of mesenchymal cells within the resected zone continued to increase while remaining

Development (2016) 143, 2066-2076 doi:10.1242/dev.131292

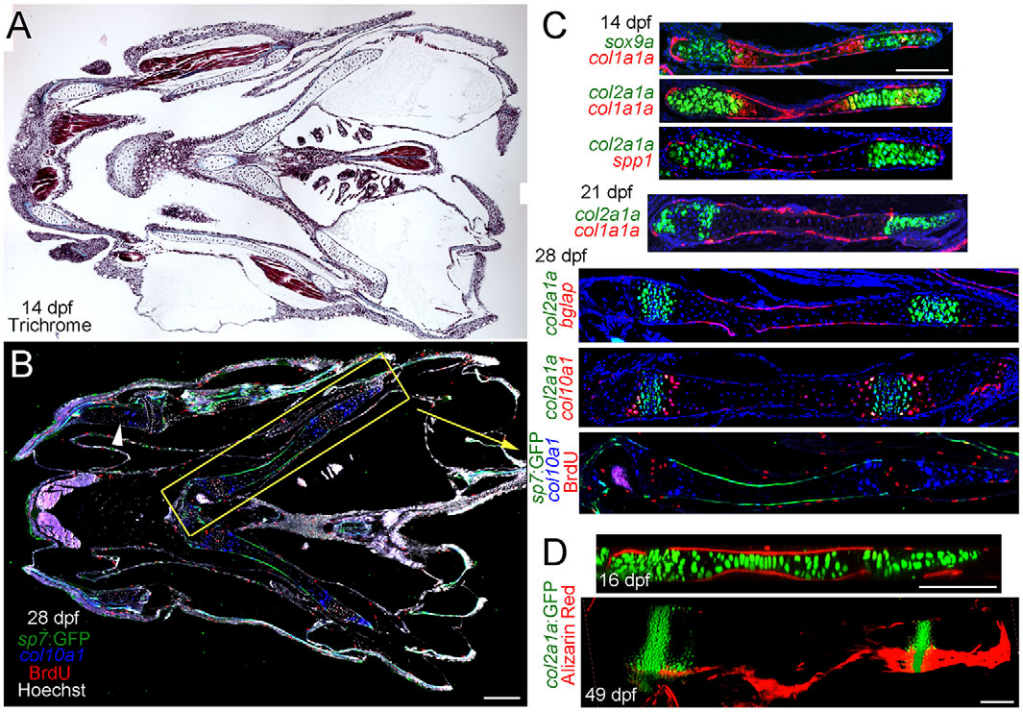

Fig. 4. Development of growth plates in juvenile zebrafish. (A) Trichrome staining of a coronal section through the juvenile fish jaw. (B) Coronal section of a 28 dpf juvenile jaw shows osteoblast precursors labeled by *sp7*:GFP, *col10a1*-expressing hypertrophic chondrocytes and BrdU^{+} proliferating cells. Hoechst labels nuclei in white. The ceratohyal cartilage (yellow box) displays a mammalian-like growth plate architecture. BrdU^{+} and *col10a1*-expressing zones are also observed in other cartilages, e.g. Meckel's (arrowhead). (C) Double fluorescent *in situ* hybridization at 14 dpf shows *sox9a* or *col2a1a* expression (green) in growth plate chondrocytes at either end of the ceratohyal cartilage and *col1a1a* expression (red) in the periosteum and a subset of chondrocytes at the hypertrophic borders. *spp1* expression (red) is confined to the periosteum. At 21 dpf, *col2a1a* continues to be expressed in two zones of chondrocytes and *col1a1a* is now largely confined to the periosteum. At 28 dpf, *bglap* is expressed exclusively in the periosteum, and *col10a1* is expressed in two stripes of hypertrophic chondrocytes surrounding each zone of *col2a1a*$^{+}$ chondrocytes. A comparison of *col2a1a* expression with BrdU reactivity shows that *col2a1a* labels proliferating chondrocytes. (D) At 16 dpr, mineralization labeled by Alizarin Red occurs exclusively within the periosteum. By 49 dpf, two growth zones of *col2a1a*^{BAC}:GFP^{+} chondrocytes persist, yet Alizarin Red^{+} mineralization remains confined to a layer covering the ceratohyal cartilage. Scale bars: 100 µm.

contiguous with the periosteum, and by 6 dpr, a few morphological chondrocytes were apparent within this mesenchyme (Fig. 5A). We note that this early cartilage formation is similarly observed at the anterior cut site of the jawbone (Fig. 1D) in which Meckel's and its associated perichondrium had been completely removed (Fig. S1), thus supporting the cartilage callus originating from periosteum surrounding bone and not perichondrium surrounding Meckel's cartilage.

We next investigated the molecular nature of the periosteal cells contributing to first mesenchyme and then chondrocytes during jawbone regeneration. In the uninjured jaw, expression of *sp7*:mCherry and *RUNX2*:GFP transgenes partially overlap, with presumptive *sp7*:mCherry^{+}/*RUNX2*:GFP^{-} early osteoblasts lining the bone and *sp7*:mCherry^{-}/*RUNX2*:GFP^{+} pre-osteoblasts located underneath (Fig. 5D,E). *sp7*:GFP^{+} bone-lining cells co-express *col1a1a*, but only some Sp7^{+} cells express *osteocalcin*:GFP, consistent with an early osteoblast identity of *sp7*-expressing cells (Fig. S2G,H). Following jawbone resection, mesenchymal cells emanating from the periosteum express *col1a1a* and *RUNX2*:GFP at 4 dpr, but not *sp7*:GFP; by contrast, periochondrial cells surrounding the remnant Meckel's cartilage are negative for *RUNX2*:GFP (Fig. 5C,F). By 7 dpr, undifferentiated mesenchyme and newly differentiating chondrocytes within the resection site remain *RUNX2*:GFP^{+}/*sp7*:GFP^{-}. We also observed extensive BrdU incorporation in mesenchyme close to the resection site, with many cells co-expressing *col1a1a* (Fig. 5C). Our data are therefore consistent with specialized bone-forming chondrocytes originating from a proliferative expansion of cells in the periosteum that express *RUNX2*:GFP and *col1a1a*, either prior to or shortly after injury.

Ihha is required for cartilage induction during jawbone regeneration

As Hh signaling has well known roles in cartilage and bone development (Long et al., 2001, 2004), we examined potential roles of this pathway in jawbone regeneration. Consistent with an involvement of Hh signaling in the formation of the cartilage callus, we observed expression of the Hh target gene *ptc2* in mesenchymal cells close to the resected region at 6 dpr (Fig. 6A). We also observed a slightly later induction of *ptc1* in *sox9a*-expressing chondrocytes at 8 dpr, and another Hh target gene, *gli1*, and *ihha* within chondrocytes at 10 dpr (Fig. 6A).

We then investigated potential requirements for Ihha signaling in jawbone regeneration by studying adult viable *ihha* mutants. As previously reported (Hammond and Schulte-Merker, 2009; Huycke et al., 2012), we found that jaw cartilage development was largely normal in *ihha*$^{-/-}$ fish, although there is a delay in perichondral bone formation that largely recovers by adulthood. In order to control for this developmental delay in bone formation, we compared jawbone regeneration in size-matched *ihha*$^{-/-}$ mutants and wild-type siblings. Strikingly, the cartilage callus was greatly reduced in *ihha*$^{-/-}$ mutants at 14 and 28 dpr (Fig. 6B,D), with mutants generating less than half the amount of repair bone by 28 dpr compared with wild-type siblings. Alizarin Red staining and bone µCT revealed that, compared with controls, the repair bone that

Development (2016) 143, 2066-2076 doi:10.1242/dev.131292

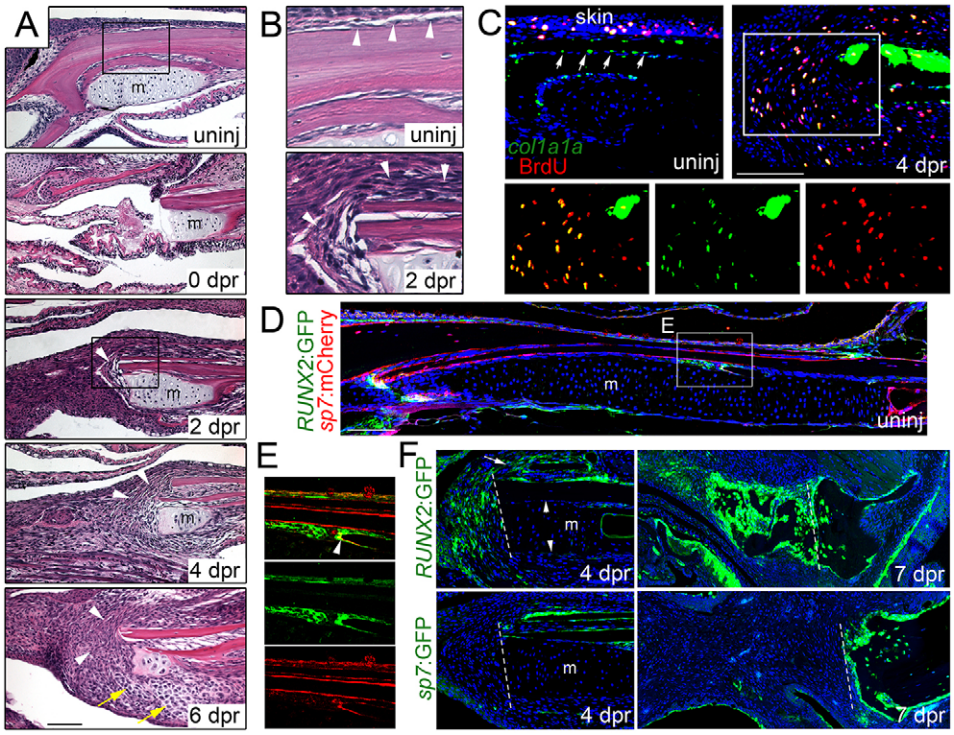

Fig. 5. Mobilization of the periosteum in response to jaw resection. (A,B) H&E staining shows the posterior site of jaw resection before and during the first week of regeneration. In the uninjured animal, the lower jawbone is lined by a thin layer of periosteum (arrowheads, see inset B). Immediately after resection (0 dpr), a small portion of Meckel's cartilage (m) remains and soft tissue collapses into the section. By 2 dpr, the periosteum (arrowheads) thickens and covers the cut surface of the bone (see inset B). The periosteum continues to expand into the resected region by 4 dpr, and 2 days later, mesenchymal cells are seen throughout the resected area and early chondrocytes can be distinguished (yellow arrows). (C) Fluorescent *in situ* hybridization for *col1a1a* (green) combined with BrdU staining (red) shows *col1a1a*$^{+}$ cells lining the uninjured jawbone periosteum (arrows), as well as the skin. At 4 dpr, *col1a1a* expression increases in the periosteum and many *col1a1a*$^{+}$ cells are seen in the mesenchyme within the resection zone. While *col1a1a*$^{+}$ cells within the uninjured periosteum are largely negative for BrdU (in contrast to those within the skin), many BrdU^{+}, *col1a1a*$^{+}$ cells are seen in the mesenchyme near the resection site (see insets for magnified images, merged and single channels). (D) Section of an uninjured adult jaw shows *sp7*:mCherry (detected by anti-mCherry antibody) in osteoblasts lining bone and *RUNX2*:GFP (detected by anti-GFP antibody) in sparse patches of periosteum. (E) Magnification of boxed region in D shows *RUNX2*:GFP expression in periosteal cells underneath *sp7*:mCherry^{+} osteoblasts. A few cells co-express both transgenes (arrowhead), consistent with early differentiating osteoblasts. (F) After resection, *RUNX2*:GFP^{+} cells are found in the periosteum (arrow) overlying the jawbone and in expanding mesenchyme at 4 dpr, but not in Meckel's cartilage or its associated periochondrium (arrowheads). By 7 dpr, both mesenchymal and early chondrocytes express *RUNX2*:GFP. By contrast, *sp7*:GFP labels the periosteum but not mesenchymal cells or chondrocytes at 4 and 7 dpr. Hoechst labels nuclei in blue. Dashed lines indicate resection sites. Scale bars: 100 µm.

formed in *ihha*$^{-/-}$ mutants contained less internal mineralization (Fig. 6B,C and Movies 2 and 3). The inability of *ihha*$^{-/-}$ mutants to make repair cartilage did not appear to be due to defects in cell proliferation, as BrdU staining at 4 dpr showed comparable numbers of proliferating mesenchymal cells between wild type and mutants (Fig. 6E,G). Furthermore, the few *col2a1a*^{BAC}:GFP^{+} chondrocytes that formed in *ihha* mutants had a similar proliferation index to those in the wild type (Fig. 6F,G). By contrast, we found greatly reduced numbers of *Sox9*$^{+}$, *col2a1a*^{BAC}:GFP^{+} cells in *ihha*$^{-/-}$ mutants at 9 dpr (Fig. 6H). Although we cannot rule out subtle effects on the proliferation of chondrocytes or their periosteal progenitors, our results are more consistent with a requirement for Ihha in the chondrogenic differentiation of periosteal cells after injury.

DISCUSSION

By studying bone regeneration in the adult zebrafish jaw, we found an important role for repair chondrocytes in directly generating thick bone during healing of large defects. Both the gene expression signature and differentiation potential of repair chondrocytes markedly differ from those of developmental chondrocytes in zebrafish, which might reflect the origin of repair chondrocytes in the periosteum – a tissue that normally produces osteoblasts during homeostasis. We also found a repair-specific requirement for Ihha signaling in generating the cartilage callus, with loss of repair cartilage in *ihha* mutants resulting in bone lacking internal mineralization. We therefore suggest that the unique context of the injured adult versus the embryo promotes a distinct cartilage differentiation program that is best adapted for rebuilding full thickness bone (Fig. 7).

Differences between bone development and regeneration in the zebrafish face

Formation of a cartilage callus is a common feature of bone fracture healing and it is generally assumed that a similar process of endochondral ossification occurs, as seen during bone development (Lieberman and Friedlaender, 2005). Our analysis of jawbone regeneration in zebrafish, however, indicates that skeletal differentiation during regeneration and development differ. First, the bulk of the zebrafish lower jawbone arises by the fusion of directly differentiating intramembranous bones, yet regeneration occurs through a cartilage intermediate. A similar phenomenon has been reported in amphibians (Ghosh et al., 1994). Second, chondrocytes within the repair callus differ from those produced during zebrafish development in that they express high levels of osteoblast-associated genes and surround themselves with

Development (2016) 143, 2066-2076 doi:10.1242/dev.131292

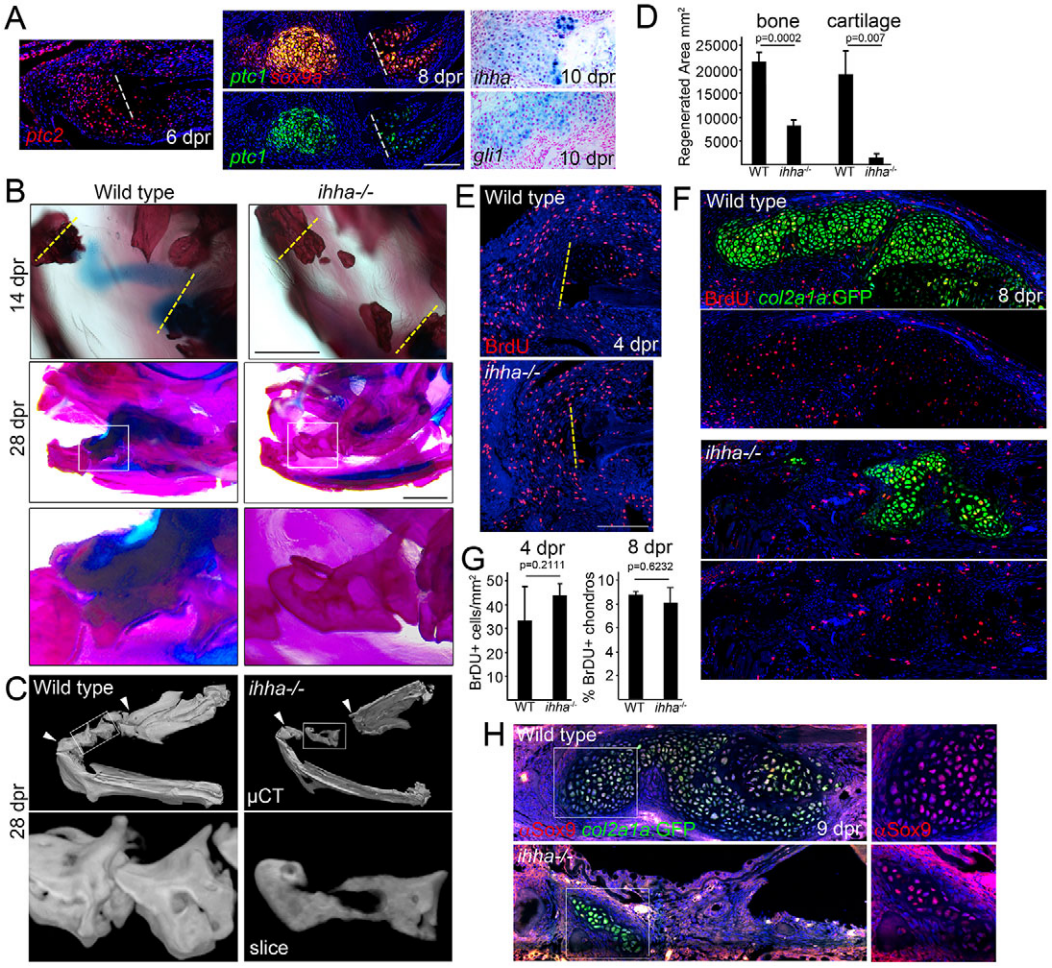

Fig. 6. Requirement of *ihha* in the generation of repair cartilage. (A) *In situ* hybridization of the regenerating jawbone shows mesenchymal expression of *ptc2* at 6 dpr, co-expression of *sox9a* and *ptc1* in the cartilage callus at 8 dpr, and *ihha* and *gli1* in the callus at 10 dpr. Dashed lines show resection sites. (B) Compared with size-matched wild-type siblings, $ihha^{-/-}$ adults show a lack of cartilage at 14 dpr. Whereas the wild type bridges the resection site with thick bone by 28 dpr, $ihha^{-/-}$ mutants have reduced and hollow bone. (C) Bone μCT shows reduced mineralization within the repair region (arrowheads). Top images are ventral views of the lower jaw and boxes show magnified images below. See also Movies 2 and 3. (D) Quantification of the area of repair bone and cartilage in the wild type and *ihha* mutants at 28 dpr. A Student's *t*-test showed statistical differences between groups. Standard errors of the mean are shown. (E) *ihha* mutants and their wild-type siblings have similar numbers of $BrdU^+$ cells in the resected regions (left of the dashed lines). (F) BrdU incorporation (red) and $col2a1a^{BAC}$:GFP labeling of chondrocytes (green, detected by anti-GFP antibody) shows reduced cartilage but similar proliferation rates in *ihha* mutants. (G) Quantification of labeled $BrdU^+$ nuclei in wild type and mutants. A Student's *t*-test showed no statistical differences at either stage. (H) Antibody staining in wild type and *ihha* mutants carrying the $col2a1a^{BAC}$:GFP transgene shows fewer chondrocytes expressing Sox9 (red) and GFP (green) in mutants versus siblings. Insets show that the few cartilage cells that form in mutants express Sox9 protein. Hoechst labels nuclei in blue. Scale bars: 1 mm in B and 100 μm in A,E.

mineralized matrix. Indeed, a major difference from mammalian bones is that zebrafish bones form primarily around the cartilage template and not within it (and hence are better referred to as periochondral). This shell mode of developmental mineralization in zebrafish makes the much different internal mineralization of cartilage during jawbone repair particularly striking. Third, Ihha is dispensable for jaw cartilage development but essential for cartilage formation in the regenerating adult jaw.

Both the type of progenitor cell and their local microenvironment differ considerably between bone development and regeneration. Whereas developmental facial chondrocytes arise from a naïve population of neural-crest-derived mesenchyme, regenerating chondrocytes appear to derive from the periosteum. As the normal function of periosteal cells is to provide a source of osteoblasts during bone homeostasis (Ono et al., 2014), an attractive possibility is that regenerating chondrocytes have an increased propensity to adopt osteoblast properties due to a memory of their osteogenic potential within the periosteum. At present, we do not know which population of periosteal cells generates repair chondrocytes. One possibility is that, as has been described in the zebrafish fin and calvaria, dedifferentiation of existing $sp7^+$ osteoblasts occurs following resection, although in the fin and calvaria, repair does not involve chondrogenesis (Knopf et al., 2011; Geurtzen et al., 2014). Alternatively, the absence of *sp7*:GFP perdurance in mesenchyme at early stages (4 dpr) could suggest that either rare *RUNX2*:GFP^+ cells, or unlabeled progenitors that rapidly express *RUNX2*:GFP, are the source of repair chondrocytes. Future lineage tracing studies of distinct periosteal cell populations will help resolve these possibilities.

Cells with dual chondrocyte and osteoblast properties during bone regeneration

During endochondral bone development in mammals, hypertrophic chondrocytes do express low levels of many osteoblast-associated

Development (2016) 143, 2066-2076 doi:10.1242/dev.131292

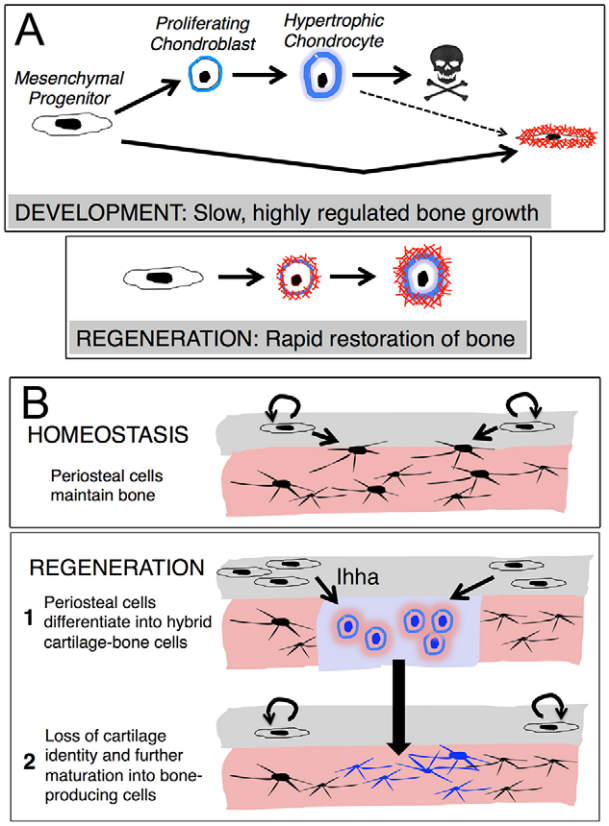

Fig. 7. Model of jawbone regeneration. (A) During endochondral bone development, chondrocyte (blue) and osteocyte (red) lineages are largely distinct. By contrast, cells co-express chondrocyte and osteoblast gene programs during lower jawbone regeneration in adult zebrafish, with chondrocyte-like cells rapidly mineralizing and maturing into osteoblasts. (B) During bone homeostasis, periosteal cells (gray layer) self-renew and contribute to new osteoblasts (black). In response to jawbone resection, Ihha signaling induces the chondrogenic differentiation of periosteal cells, with these repair chondrocytes (blue) maturing into bone-producing cells.

genes (e.g. *Runx2* and *Spp1*) and produce a calcified matrix (Dy et al., 2012). By contrast, zebrafish developmental chondrocytes largely fail to calcify. Although the calcification of mammalian hypertrophic chondrocytes appears reminiscent of what we observe during zebrafish jawbone regeneration, there are important differences. Repair chondrocytes in fish express *runx2b* and *col1a1a* earlier than *col10a1* and at levels comparable to those seen in directly differentiating osteoblasts, as opposed to the weaker and later expression of osteoblast markers only in *Col10a1*$^{+}$ hypertrophic chondrocytes of mammals (Dy et al., 2012). Repair chondrocytes, but not developmental chondrocytes, in the zebrafish jaw also express the later osteoblast markers *spp1* and *bglap*. Interestingly, *Bglap* is also expressed in chondrocytes during mammalian fracture repair (Scammell and Roach, 1996; Bahney et al., 2014), suggesting that chondrocytes during mammalian bone repair might also have increased osteoblast characteristics compared with their developmental counterparts. Of note, what we observe during jawbone regeneration differs to some extent from the reported transdifferentiation of hypertrophic chondrocytes into osteocytes during mammalian endochondral development (Shimomura et al., 1975; Mayne et al., 1976; von der Mark and von der Mark, 1977; Yang et al., 2014; Zhou et al., 2014). Although hypertrophic chondrocytes appear to shut down their chondrocyte expression program and then only later upregulate an osteoblast program in the growth plate, zebrafish repair chondrocytes co-express chondrocyte and osteoblast genes at initial stages.

While cells co-expressing high levels of chondrocyte and osteoblast genes are most prominent during adult repair, these cells bear a striking resemblance to those described for ‘chondroid bone’. This tissue has a long history in the literature, being described as a rare type of avascular bone thought to arise directly from the mineralization of cartilage (Beresford, 1981; Goret-Nicaise, 1984; Huysseune and Verraes, 1986). During mammalian development, chondroid bone contributes to the baculum and mandibular condyle (Beresford, 1975; Beresford and Burkart, 1977; Mizoguchi et al., 1993; Herdina et al., 2010), and there are numerous histological studies implicating chondroid bone in fracture repair (Pritchard and Ruzicka, 1950; Neufeld, 1985; Yasui et al., 1997), including a study on jawbone fracture repair in goldfish (Moss, 1962). As with the repair chondrocytes we describe for zebrafish jawbone regeneration, immunohistochemistry of chondroid bone has revealed colocalization of type I and II collagen and BGLAP protein, with chondrocyte-like cells embedded in mature bone (Scammell and Roach, 1996). Our data extend these findings to show that the same repair cells can produce all these proteins, and that chondroid bone is abundantly produced from the periosteum during large-scale bone regeneration.

In contrast to the pervasive dogma of distinct chondrocyte and osteoblast lineages, emerging evidence suggests that skeletal fates are quite plastic during development. For example, early osteochondroprogenitors are thought to transiently co-express *Sox9* and *Runx2* (Eames et al., 2004), as well as *Col2a1* (Ono et al., 2014). Osteoblasts in the calvaria of avians also express low levels of *Col2a1* (but not Col2a1 protein) (Abzhanov et al., 2007) and in zebrafish, developmental chondrocytes transiently express low levels of *col1a2* and *sp7* (Hammond and Schulte-Merker, 2009). In addition, mammalian growth plate chondrocytes in which *Sox9* has been deleted in the *Aggrecan*$^{+}$ lineage inappropriately express high levels of *Col1a1*, *Runx2* and *Sp7* (Dy et al., 2012). Chondrocytes and osteoblasts might thus represent a continuum of cell types, as opposed to discrete entities (Apschner et al., 2011). One possibility then is that repair chondrocytes and developmental hypertrophic chondrocytes simply occupy different positions in the cartilage-bone spectrum. For example, the precise organization of the developing growth plate might help to limit the osteogenic potential of hypertrophic chondrocytes, with the injury microenvironment and less organized nature of the repair cartilage callus contributing to its increased osteoblastic character.

That the nature and role of cartilage would differ between bone development and repair also makes sense from a functional perspective. During the development of cartilage-replacement bones, a fetal template has increased tremendously in size by adulthood, which is accomplished by a tightly regulated conversion of growth plates into bone by a distinct source of osteoblasts (Maes et al., 2010). By contrast, when confronted with a large bone injury, the goal would be to re-establish rigidity as quickly as possible to ensure organismal survival. Perhaps generating unique repair chondrocytes that first bridge the wound and then directly produce mineralized matrix allows a more rapid restoration of thick bone to stabilize the jaw.

A repair-specific role of Ihha in inducing the cartilage callus from the periosteum

A feature of bone repair in both mammals and zebrafish is that periosteal cells, which produce only osteoblasts during normal homeostasis, now also produce chondrocytes in response to injury.

Development (2016) 143, 2066-2076 doi:10.1242/dev.131292

Here, we show that Ihha is essential for the periosteum to efficiently produce chondrocytes during jawbone regeneration. Whereas Ihh promotes the proliferation of chondrocytes in mammalian growth plates (Long et al., 2001), our data are more consistent with Ihha inducing chondrogenic differentiation during zebrafish jawbone repair. Although the expression of *ptc2* before overt cartilage differentiation is consistent with a role for Ihha in cartilage induction, we were only able to detect *ihha* expression in chondrocytes themselves. This failure to detect *ihha* expression in pre-chondrogenic cells might reflect transient or low levels of ligand expression at earlier stages. Nonetheless, future studies focused on more sensitive detection techniques for *ihha* expression and selective inhibition of Hh signaling at later chondrogenic stages will be needed to rule out an additional role for Ihha in maintaining repair chondrocytes.

Our genetic data indicate that *ihha* has a specific requirement for cartilage induction during repair but not development. This might be explained by redundant roles for the *ihhb* co-ortholog during development, as we detected low levels of *ihhb* expression in both developmental and repair chondrocytes (Fig. S2D and data not shown). Compensation by Ihhb might also account for the production of small amounts of repair cartilage in *ihha* mutants. Alternatively, Shh signaling could be performing the analogous function to Ihha in inducing cartilage during development. Indeed, combined loss of *shha* and *shhb*, or the *smo* receptor, results in a near complete loss of craniofacial cartilage in zebrafish larvae (Eberhart et al., 2006).

One feature of the *ihha* mutant is that, despite the lack of a cartilage callus after injury, some regenerated bone still forms. However, mutant repair bone is significantly reduced and lacking in internal mineralization compared with controls. This observation suggests that, although not strictly required for bone repair, the cartilage callus is especially important for generating thick, internal bone. The reduction in repair bone might also reflect a role for Ihha in intramembranous ossification (Hammond and Schulte-Merker, 2009; Huycke et al., 2012). Perhaps, in the absence of Ihha, periosteal cells that would otherwise have made chondrocytes instead make osteoblasts, with these osteoblasts generating cortical bone via intramembranous ossification instead of the internal bone produced directly by the cartilage callus. Alternatively, different subsets of cells within the periosteum could generate osteoblasts and chondrocytes during jawbone repair, with those periosteal cells that would have made chondrocytes simply failing to differentiate in *ihha* mutants. In the future, transgenic lines that allow long-term lineage tracing of specific subsets of periosteal cells will help us to determine whether Ihha signaling diverts cells that would normally make osteoblasts during homeostasis towards making chondrocytes during large-scale bone repair.

MATERIALS AND METHODS

Zebrafish strains

All procedures were approved by the University of Southern California Institutional Animal Care and Use Committee. Zebrafish lines include *ihha*^{hu2131} (Hammond and Schulte-Merker, 2009), *Tg(Has.RUNX2:EGFP)*^{zf259} (Kague et al., 2012), *Tg(sp7:EGFP)*^{b1212} (DeLaurier et al., 2010), *Tg(col2a1a*$_{BAC}$*:GFP)*^{el483} (Askary et al., 2015), *Tg(Ola.Sp7:CreERT2-P2A-mCherry)* (i.e. sp7:mCherry) and *Tg(Ola.Osteocalcin.1:EGFP)* (Knopf et al., 2011).

Jawbone resection

Resections were performed on anesthetized 4-12 month zebrafish using Vannas spring scissors (Fine Science Tools) and chemically etched tungsten needles. An anterior cut was made in the dentary bone adjacent to the mandibular symphysis and a posterior cut where the maxillary barbel inserts into the upper jaw. Connective tissue was scored and bone removed with forceps while leaving the skin, which closes up within a few minutes. Fish were then transferred to fresh water. No ill effects of jaw resection were observed.

Skeletal analysis

An acid-free cartilage and bone staining protocol was used (Askary et al., 2015). Live bone staining was performed by bathing fish in 0.01% Alizarin Red solution for 1 h (16 dpf) or overnight (49 dpf and adults). Excess dye was removed by several rinses in system water.

Paraffin embedding and histology

Following euthanasia, larvae or isolated adult heads were fixed in 4% paraformaldehyde for 1 week, decalcified in 20% EDTA for 10 days and embedded in paraffin. Decalcification was omitted for 14 dpf larvae and reduced to 5 days for 21-30 dpf stages. 5 µm sections were cut on a Shandon Finesse Me+ microtome (cat no. 77500102) and collected on superfrost plus slides (Thermo Fisher Scientific). H&E staining (VWR) and trichrome staining (Newcomer Supply) were according to the manufacturer's instructions.

In situ hybridization, immunohistochemistry and BrdU treatment

Fluorescent *in situ* hybridization (ISH) on paraffin sections was carried out as described (https://wiki.zfin.org/display/prot/3+color+Fluorescent+in+situ+on+sections). For colorimetric ISH, digoxigenin-labeled riboprobes were detected with an anti-digoxigenin alkaline phosphatase antibody (1:2000, Roche, 11093274910) followed by visualization with Nitro Blue tetrazolium and 5-bromo-4-chloro-3-indolyl-phosphate. Except for *sox9a* (Yan et al., 2005), probe templates were amplified (primer sequences in Table S1) and cloned into pCR-BluntII-TOPO (Invitrogen), followed by linearization and *in vitro* transcription following the manufacturer's instructions (Roche Life Science, 11175025910). For anti-BrdU or anti-Sox9 antibodies, antigen retrieval was performed by steaming the slides in a steamer set (IHC World, IW-1102) for 35 min in citrate buffer (pH 6.0) followed by cooling to room temperature. Immunohistochemistry was performed according to Stewart et al. (2014) with the exception of blocking with 2% normal goat serum (Jackson ImmunoResearch, 005-000-121). Primary antibodies include rat anti-BrdU (1:100, Bio-Rad, MCA2060GA), rabbit anti-Sox9a (1:500, GeneTex, GTX128370), mouse anti-Col2a1 (1:50, DSHB-II-II6B3), rabbit anti-Col1a1a (1:100, GeneTex, GTX128242), rabbit anti-Osterix (1:500, Santa Cruz Biotechnology, sc-22536-R), rabbit anti-GFP (1:500, Torrey Pines, TP401) and mouse anti-GFP (1:50, Sigma Aldrich, 11814460001). Alexa Fluor secondary antibodies were used. Larval or adult fish were treated with 4.5 mg/ml BrdU (Sigma Aldrich, B5002) by bath application for 1 h, followed by two washes, euthanasia and fixation in 4% paraformaldehyde.

Imaging

Skeletons and bright-field images of H&E, Trichrome and colorimetric *in situ* hybridizations were acquired with a Leica S8 APO or DM2500 compound microscope. Multiple images were focus stacked using Adobe Photoshop CS5. Fluorescent images were acquired with Zeiss LSM5, LSM780 or LSM 800 confocal microscopes, and maximum intensity projections generated using ZEN. µCT was performed on paraffin-embedded Alcian Blue- and Alizarin Red-stained jaws, in air on a XT-H-225S-T micro-CT scanner (Nikon Metrology, Brighton, MI) at 3 µm voxel volume. A molybdenum target was used with no additional filtration of the beam. Raw data was reconstructed in CT-Pro-3D v4.3.4 and rendered on VG-StudioMax v2.2 (Volume Graphics, Heidelberg, Germany).

Quantification

For cell proliferation, we counted BrdU^{+} nuclei/mm^{2} at 4 dpr and BrdU^{+} cells as percentage of *col2a1a*$_{BAC}$:GFP^{+} cells at 8 dpr. For bone and cartilage defects in *ihha* mutants, the area of Alizarin Red^{+} bone and Alcian Blue^{+} cartilage was calculated using Fiji. Significance was determined by Student's *t*-test. See Table S2 for experimental numbers.

Acknowledgements
We thank Megan Matsutani and Jennifer DeKoeyer Crump for fish care, Shannon Fisher for the *RUNX2*:GFP line, Bino Varghese and Seth Ruffins for assistance with μCT, and Jay Lieberman and Andy McMahon for advice.

Competing interests
The authors declare no competing or financial interests.

Author contributions
S.P., S.S., D.G. and A.d.M.T. performed the experiments. S.P., D.G., F.V.M. and J.G.C. designed the experiments, interpreted results and wrote the manuscript.

Funding
Funding was from a California Institute for Regenerative Medicine (CIRM) New Investigator Award to J.G.C.; the National Institutes of Health [R21 DE023899 to J.G.C.; R21 AR064462 to F.V.M.]; and a University of Southern California Regenerative Medicine Initiative Award to F.V.M. and J.G.C. Deposited in PMC for release after 12 months.

Supplementary information
Supplementary information available online at
http://dev.biologists.org/lookup/suppl/doi:10.1242/dev.131292/-/DC1

References

Abzhanov, A., Rodda, S. J., McMahon, A. P. and Tabin, C. J. (2007). Regulation of skeletogenic differentiation in cranial dermal bone. *Development* **134**, 3133-3144.
Apschner, A., Schulte-Merker, S. and Witten, P. E. (2011). Not all bones are created equal - using zebrafish and other teleost species in osteogenesis research. *Methods Cell Biol.* **105**, 239-255.
Askary, A., Mork, L., Paul, S., He, X., Izuhara, A. K., Gopalakrishnan, S., Ichida, J. K., McMahon, A. P., Dabizljevic, S., Dale, R. et al. (2015). Iroquois proteins promote skeletal joint formation by maintaining chondrocytes in an immature state. *Dev. Cell* **35**, 358-365.
Bahney, C. S., Hu, D. P., Taylor, A. J., Ferro, F., Britz, H. M., Hallgrimsson, B., Johnstone, B., Miclau, T. and Marcucio, R. S. (2014). Stem cell-derived endochondral cartilage stimulates bone healing by tissue transformation. *J. Bone Miner. Res.* **29**, 1269-1282.
Baht, G. S., Silkstone, D., Nadesan, P., Whetstone, H. and Alman, B. A. (2014). Activation of hedgehog signaling during fracture repair enhances osteoblastic-dependent matrix formation. *J. Orthop. Res.* **32**, 581-586.
Beresford, W. A. (1975). Schemes of zonation in the mandibular condyle. *Am. J. Orthod.* **68**, 189-195.
Beresford, W. A. (1981). *Chondroid Bone, Secondary Cartilage, and Metaplasia*. Baltimore, MD: Urban & Schwarzenberg.
Beresford, W. A. and Burkart, S. (1977). The penile bone and anterior process of the rat in scanning electron microscopy. *J. Anat.* **124**, 589-597.
Brockes, J. P. (1997). Amphibian limb regeneration: rebuilding a complex structure. *Science* **276**, 81-87.
DeLaurier, A., Eames, B. F., Blanco-Sánchez, B., Peng, G., He, X., Swartz, M. E., Ullmann, B., Westerfield, M. and Kimmel, C. B. (2010). Zebrafish sp7:EGFP: a transgenic for studying otic vesicle formation, skeletogenesis, and bone regeneration. *Genesis* **48**, 505-511.
Dy, P., Wang, W., Bhattaram, P., Wang, Q., Wang, L., Ballock, R. T. and Lefebvre, V. (2012). Sox9 directs hypertrophic maturation and blocks osteoblast differentiation of growth plate chondrocytes. *Dev. Cell* **22**, 597-609.
Eames, B. F., Sharpe, P. T. and Helms, J. A. (2004). Hierarchy revealed in the specification of three skeletal fates by Sox9 and Runx2. *Dev. Biol.* **274**, 188-200.
Eberhart, J. K., Swartz, M. E., Crump, J. G. and Kimmel, C. B. (2006). Early Hedgehog signaling from neural to oral epithelium organizes anterior craniofacial development. *Development* **133**, 1069-1077.
Geurtzen, K., Knopf, F., Wehner, D., Huitema, L. F. A., Schulte-Merker, S. and Weidinger, G. (2014). Mature osteoblasts dedifferentiate in response to traumatic bone injury in the zebrafish fin and skull. *Development* **141**, 2225-2234.
Ghosh, S., Thorogood, P. and Ferretti, P. (1994). Regenerative capability of upper and lower jaws in the newt. *Int. J. Dev. Biol.* **38**, 479-490.
Goret-Nicaise, M. (1984). Identification of collagen type I and type II in chondroid tissue. *Calcif. Tissue Int.* **36**, 682-689.
Goss, R. J. and Stagg, M. W. (1958). Regeneration in lower jaws of newts after excision of the intermandibular regions. *J. Exp. Zool.* **137**, 1-11.
Graver, H. T. (1978). Re-regeneration of lower jaws and the dental lamina in adult urodeles. *J. Morphol.* **157**, 269-279.
Hall, B. K. and Hanken, J. (1985). Repair of fractured lower jaws in the spotted salamander: do amphibians form secondary cartilage? *J. Exp. Zool.* **233**, 359-368.
Hammond, C. L. and Schulte-Merker, S. (2009). Two populations of endochondral osteoblasts with differential sensitivity to Hedgehog signalling. *Development* **136**, 3991-4000.
Herdina, A. N., Herzig-Straschil, B., Hilgers, H., Metscher, B. D. and Plenk, H. Jr. (2010). Histomorphology of the penis bone (Baculum) in the gray long-eared bat Plecotus austriacus (Chiroptera, Vespertilionidae). *Anat. Rec.* **293**, 1248-1258.
Huang, C., Tang, M., Yehling, E. and Zhang, X. (2014). Overexpressing sonic hedgehog peptide restores periosteal bone formation in a murine bone allograft transplantation model. *Mol. Ther.* **22**, 430-439.
Huycke, T. R., Eames, B. F. and Kimmel, C. B. (2012). Hedgehog-dependent proliferation drives modular growth during morphogenesis of a dermal bone. *Development* **139**, 2371-2380.
Huysseune, A. and Verraes, W. (1986). Chondroid bone on the upper pharyngeal jaws and neurocranial base in the adult fish Astatotilapia elegans. *Am. J. Anat.* **177**, 527-535.
Iovine, M. K. (2007). Conserved mechanisms regulate outgrowth in zebrafish fins. *Nat. Chem. Biol.* **3**, 613-618.
Kague, E., Gallagher, M., Burke, S., Parsons, M., Franz-Odendaal, T. and Fisher, S. (2012). Skeletogenic fate of zebrafish cranial and trunk neural crest. *PLoS ONE* **7**, e47394.
Knopf, F., Hammond, C., Chekuru, A., Kurth, T., Hans, S., Weber, C. W., Mahatma, G., Fisher, S., Brand, M., Schulte-Merker, S. et al. (2011). Bone regenerates via dedifferentiation of osteoblasts in the zebrafish fin. *Dev. Cell* **20**, 713-724.
Lieberman, J. R. and Friedlaender, G. E. (2005). *Bone Regeneration and Repair: Biology and Clinical Applications*. Totowa, NJ: Humana Press.
Long, F., Zhang, X. M., Karp, S., Yang, Y. and McMahon, A. P. (2001). Genetic manipulation of hedgehog signaling in the endochondral skeleton reveals a direct role in the regulation of chondrocyte proliferation. *Development* **128**, 5099-5108.
Long, F., Chung, U.-I., Ohba, S., McMahon, J., Kronenberg, H. M. and McMahon, A. P. (2004). Ihh signaling is directly required for the osteoblast lineage in the endochondral skeleton. *Development* **131**, 1309-1318.
Mackie, E. J., Ahmed, Y. A., Tatarczuch, L., Chen, K.-S. and Mirams, M. (2008). Endochondral ossification: how cartilage is converted into bone in the developing skeleton. *Int. J. Biochem. Cell Biol.* **40**, 46-62.
Maes, C., Kobayashi, T., Selig, M. K., Torrekens, S., Roth, S. I., Mackem, S., Carmeliet, G. and Kronenberg, H. M. (2010). Osteoblast precursors, but not mature osteoblasts, move into developing and fractured bones along with invading blood vessels. *Dev. Cell* **19**, 329-344.
Mayne, R., Vail, M. S., Mayne, P. M. and Miller, E. J. (1976). Changes in type of collagen synthesized as clones of chick chondrocytes grow and eventually lose division capacity. *Proc. Natl. Acad. Sci. USA* **73**, 1674-1678.
Mizoguchi, I., Nakamura, M., Takahashi, I., Sasano, Y., Kagayama, M. and Mitani, H. (1993). Presence of chondroid bone on rat mandibular condylar cartilage. An immunohistochemical study. *Anat. Embryol.* **187**, 9-15.
Moss, M. L. (1962). Studies of the acellular bone of teleost fish. II. Response to fracture under normal and acalcemic conditions. *Acta Anat.* **48**, 46-60.
Murao, H., Yamamoto, K., Matsuda, S. and Akiyama, H. (2013). Periosteal cells are a major source of soft callus in bone fracture. *J. Bone Miner. Metab.* **31**, 390-398.
Neufeld, D. A. (1985). Bone healing after amputation of mouse digits and newt limbs: implications for induced regeneration in mammals. *Anat. Rec.* **211**, 156-165.
Ono, N., Ono, W., Nagasawa, T. and Kronenberg, H. M. (2014). A subset of chondrogenic cells provides early mesenchymal progenitors in growing bones. *Nat. Cell Biol.* **16**, 1157-1167.
Ortuno, M. J., Susperregui, A. R. G., Artigas, N., Rosa, J. L. and Ventura, F. (2013). Osterix induces Col1a1 gene expression through binding to Sp1 sites in the bone enhancer and proximal promoter regions. *Bone* **52**, 548-556.
Pritchard, J. J. and Ruzicka, A. J. (1950). Comparison of fracture repair in the frog, lizard and rat. *J. Anat.* **84**, 236-261.
Scammell, B. E. and Roach, H. I. (1996). A new role for the chondrocyte in fracture repair: endochondral ossification includes direct bone formation by former chondrocytes. *J. Bone Miner. Res.* **11**, 737-745.
Shimomura, Y., Yoneda, T. and Suzuki, F. (1975). Osteogenesis by chondrocytes from growth cartilage of rat rib. *Calcif. Tissue Res.* **19**, 179-187.
Singh, S. P., Holdway, J. E. and Poss, K. D. (2012). Regeneration of amputated zebrafish fin rays from de novo osteoblasts. *Dev. Cell* **22**, 879-886.
St-Jacques, B., Hammerschmidt, M. and McMahon, A. P. (1999). Indian hedgehog signaling regulates proliferation and differentiation of chondrocytes and is essential for bone formation. *Genes Dev.* **13**, 2072-2086.
Stewart, S., Gomez, A. W., Armstrong, B. E., Henner, A. and Stankunas, K. (2014). Sequential and opposing activities of Wnt and BMP coordinate zebrafish bone regeneration. *Cell Rep.* **6**, 482-498.
von der Mark, K. and von der Mark, H. (1977). The role of three genetically distinct collagen types in endochondral ossification and calcification of cartilage. *J. Bone Joint Surg. Br.* **59-B**, 458-464.
Wang, X., He, H., Tang, W., Zhang, X. A., Hua, X. and Yan, J. (2012). Two origins of blastemal progenitors define blastemal regeneration of zebrafish lower jaw. *PLoS ONE* **7**, e45380.

Development (2016) 143, 2066-2076 doi:10.1242/dev.131292

Yan, Y.-L., Willoughby, J., Liu, D., Crump, J. G., Wilson, C., Miller, C. T., Singer, A., Kimmel, C., Westerfield, M. and Postlethwait, J. H. (2005). A pair of Sox: distinct and overlapping functions of zebrafish sox9 co-orthologs in craniofacial and pectoral fin development. *Development* **132**, 1069-1083.

Yang, L., Tsang, K. Y., Tang, H. C., Chan, D. and Cheah, K. S. E. (2014). Hypertrophic chondrocytes can become osteoblasts and osteocytes in endochondral bone formation. *Proc. Natl. Acad. Sci. USA* **111**, 12097-12102.

Yasui, N., Sato, M., Ochi, T., Kimura, T., Kawahata, H., Kitamura, Y. and Nomura, S. (1997). Three modes of ossification during distraction osteogenesis in the rat. *J. Bone Joint Surg. Br.* **79**, 824-830.

Yu, Y. Y., Lieu, S., Lu, C. and Colnot, C. (2010). Bone morphogenetic protein 2 stimulates endochondral ossification by regulating periosteal cell fate during bone repair. *Bone* **47**, 65-73.

Zhou, X., von der Mark, K., Henry, S., Norton, W., Adams, H. and de Crombrugghe, B. (2014). Chondrocytes transdifferentiate into osteoblasts in endochondral bone during development, postnatal growth and fracture healing in mice. *PLoS Genet.* **10**, e1004820.

Zou, S., Chen, T., Wang, Y., Tian, R., Zhang, L., Song, P., Yang, S., Zhu, Y., Guo, X., Huang, Y. et al. (2014). Mesenchymal stem cells overexpressing Ihh promote bone repair. *J. Orthop. Surg. Res.* **9**, 102.

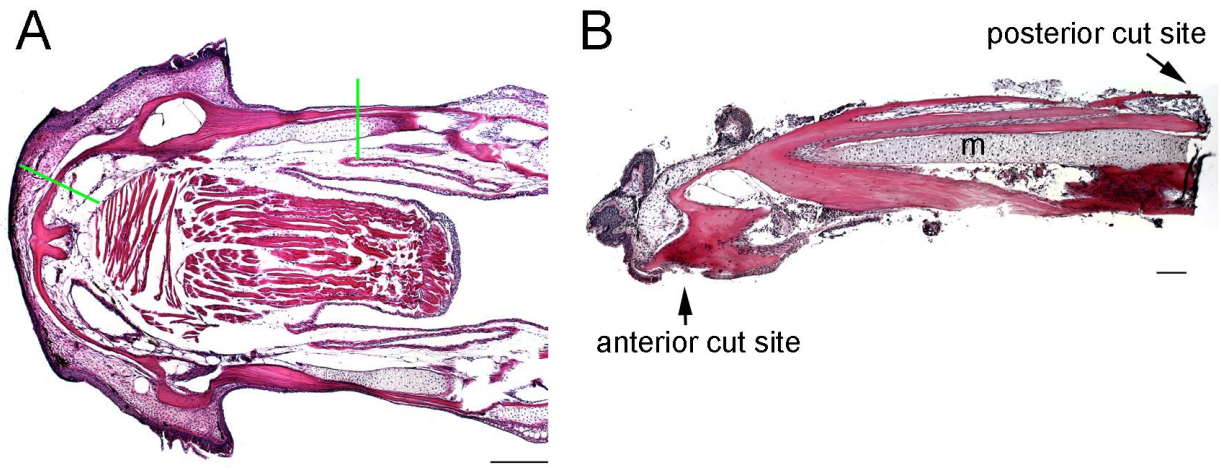

Fig. S1. Extent of lower jaw resections.

(A) Coronal section of un-resected adult lower jaw stained with H&E. Green lines show where resection cuts are made. Anterior is to the left. (B) Histological section through the tissue that was removed showing the extent of bone removed and complete removal of the distal end of Meckel's cartilage (m). Scale bars: A, 1 mm; B, 100 microns.

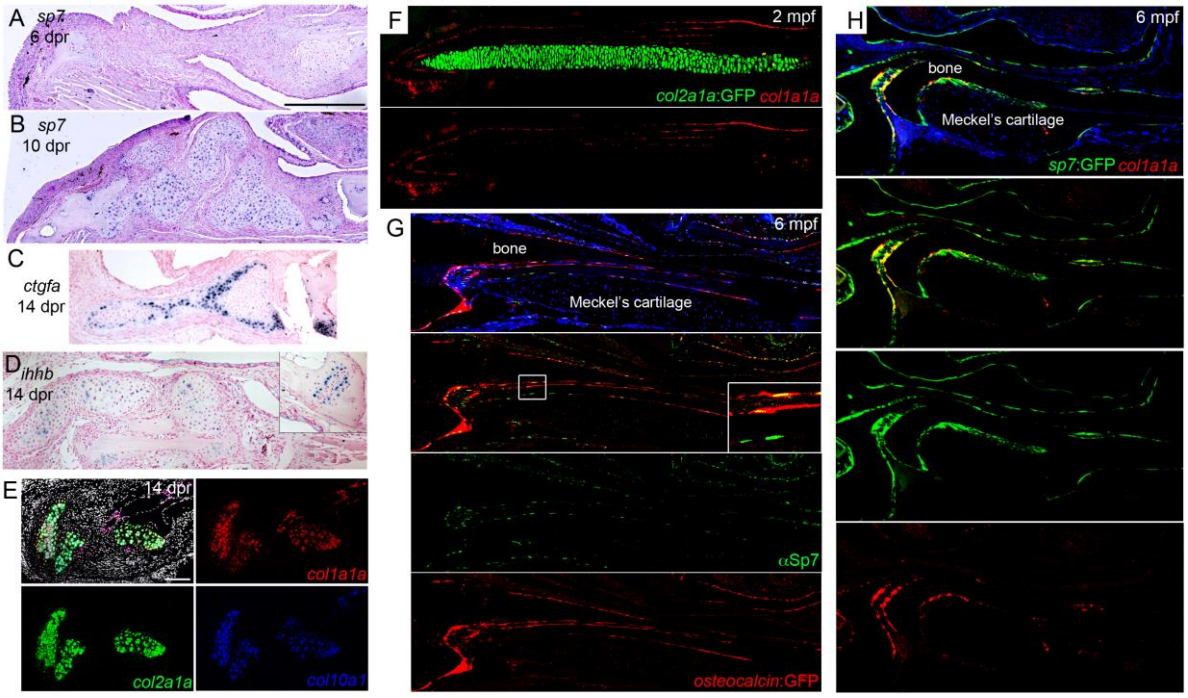

Fig. S2. Gene expression in the cartilage callus and adult jaw.

(A-D) Colorimetric RNA in situ hybridization shows gene expression in the cartilage callus. The expression of *sp7* is not yet visible in the mesenchyme at 6 dpr and evident in the cartilage callus by 10 dpr. At 14 dpr, *ctgfa* is expressed in a subset of chondrocytes within the callus. Also at 14 dpr, *ihhb* is expressed weakly in some repair chondrocytes; inset shows stronger expression in the remnant growth plate of the ceratohyal cartilage. (E) Three-color fluorescent in situ hybridization shows co-expression of *col1a1a* (red), *col2a1a* (green), and *col10a1* (blue) within repair chondrocytes at 10 dpr. Note the similar level of expression of *col1a1a* in the bone (top right). Nuclei are detected with Hoechst (white). (F) Transgenic *col2a1a*^{BAC}:GFP fish have distinct and non-overlapping expression of GFP in Meckel's cartilage and *col1a1a* in periosteum at 2 mpf. (G) A subset of Sp7+ cells (green, detected by anti-

Sp7 antibody) also express an *osteocalcin:*GFP transgene (red, detected by anti-GFP antibody). Inset corresponds to boxed region and shows both Sp7-only cells and Sp7+/*osteocalcin*:GFP+ cells. Note nuclear Sp7 localization compared to cytoplasmic and nuclear GFP. (H) A subset of *sp7:*GFP+ cells express *col1a1a*. Scale bars = 100 microns.

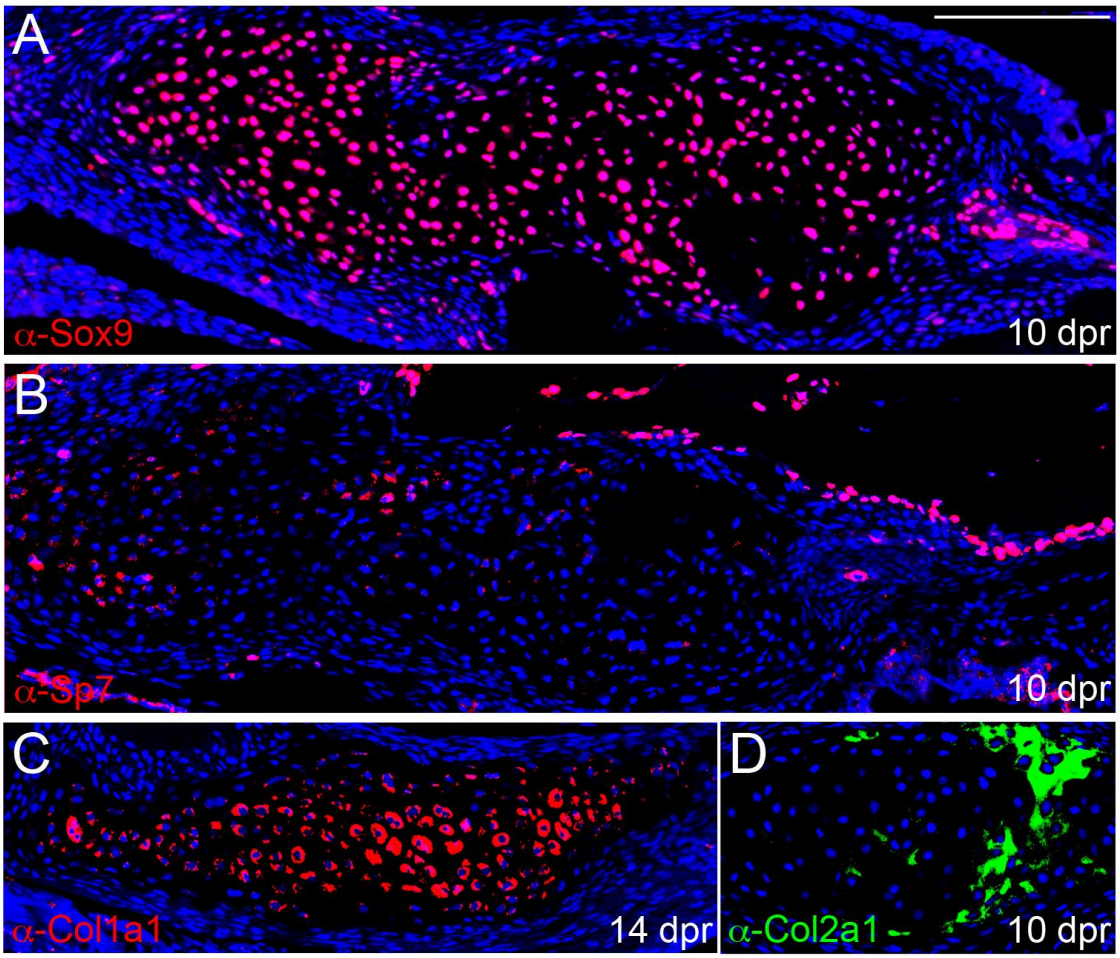

Fig. S3. Protein expression in the cartilage callus.

(A-D) Immunofluorescent assays on sections show protein expression of Sox9, Sp7, Col1a1, and Col2a1 within the cartilage callus. Nuclei are labeled with Hoechst (blue). Scale bar = 100 microns.

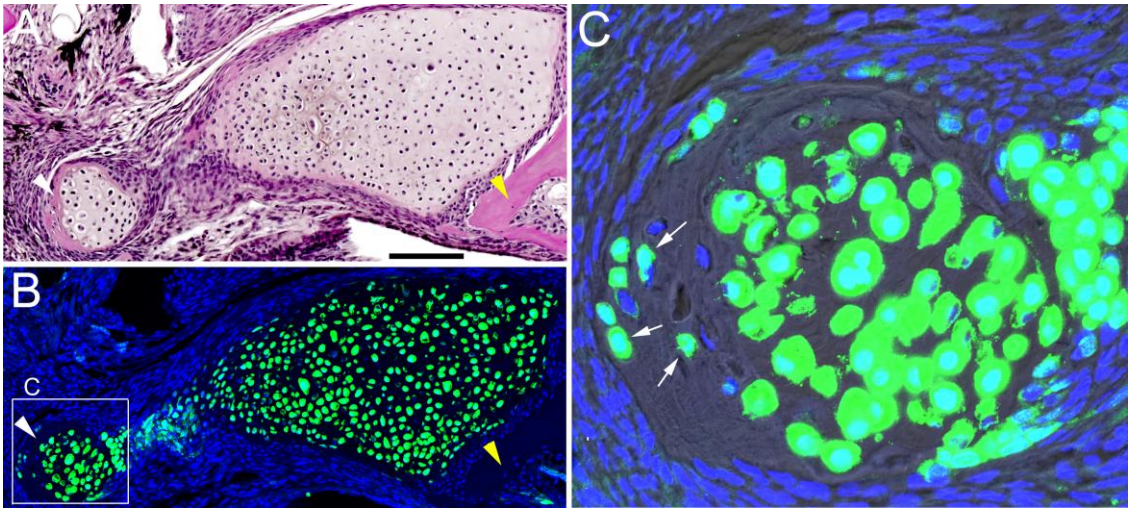

Fig. S4. Contribution of *col2a1a*^{BAC}:GFP-derived cells to bone.

(A) H&E staining at 30 dpr shows remnant cartilage surrounded by bone (white arrowhead) which has a similar appearance to bone on the right (yellow arrowhead). (B) An adjacent section from this *col2a1a*^{BAC}:GFP animal was processed for anti-GFP staining (green). Hoescht labels nuclei in blue. (C) Magnification shows that GFP+ cells are embedded in bone (arrows). A Normarski channel is included to show bone matrix. Scale bar = 100 microns.

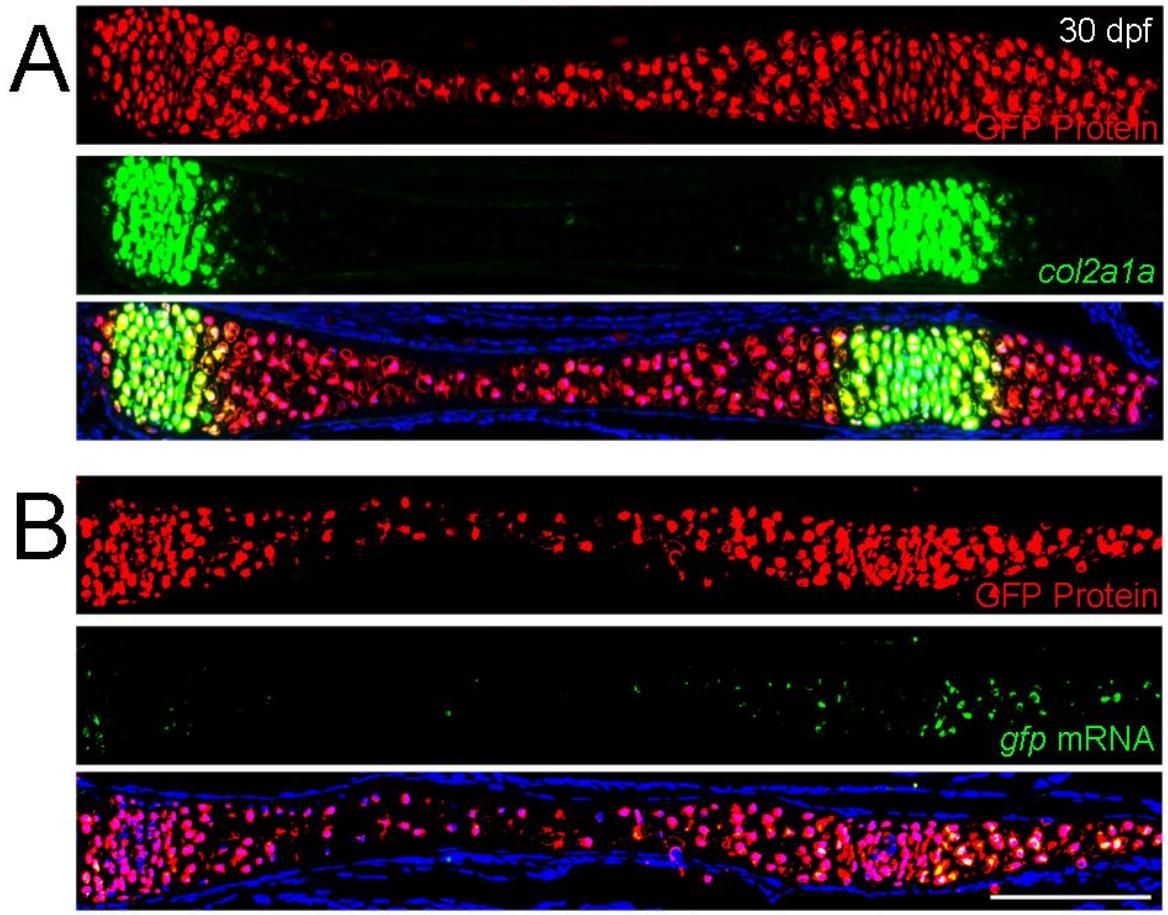

Fig. S5. Perdurance of GFP in developing cartilage.

(A and B) Sections of the ceratohyal cartilage in 30 dpf *col2a1a*^{BAC}:GFP juvenile zebrafish. Anti-GFP staining (red) compared to endogenous *col2a1a* RNA (green, A) or GFP RNA (green, B) shows that cells retain GFP protein after they shut down expression of *col2a1a* or GFP message. Scale bar = 100 microns.

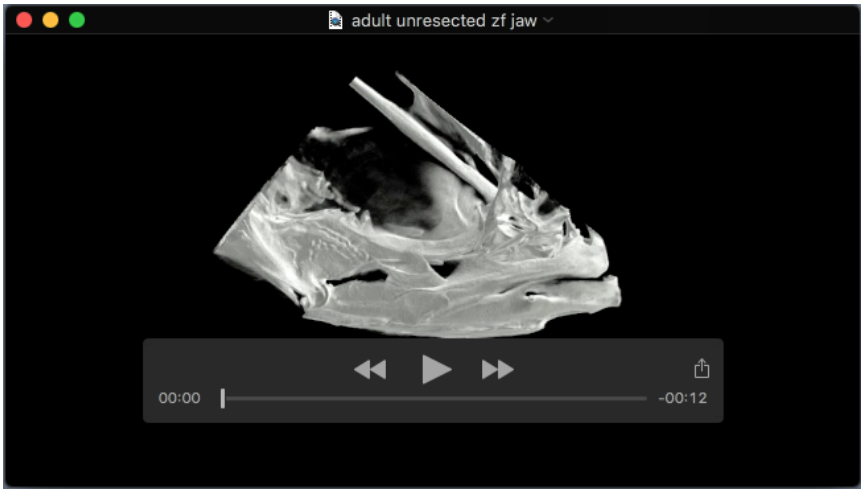

Movie 1. Volume reconstruction of µCT scans showing anatomy of an uninjured adult zebrafish lower jawbone (highlighted to discern from other structures).

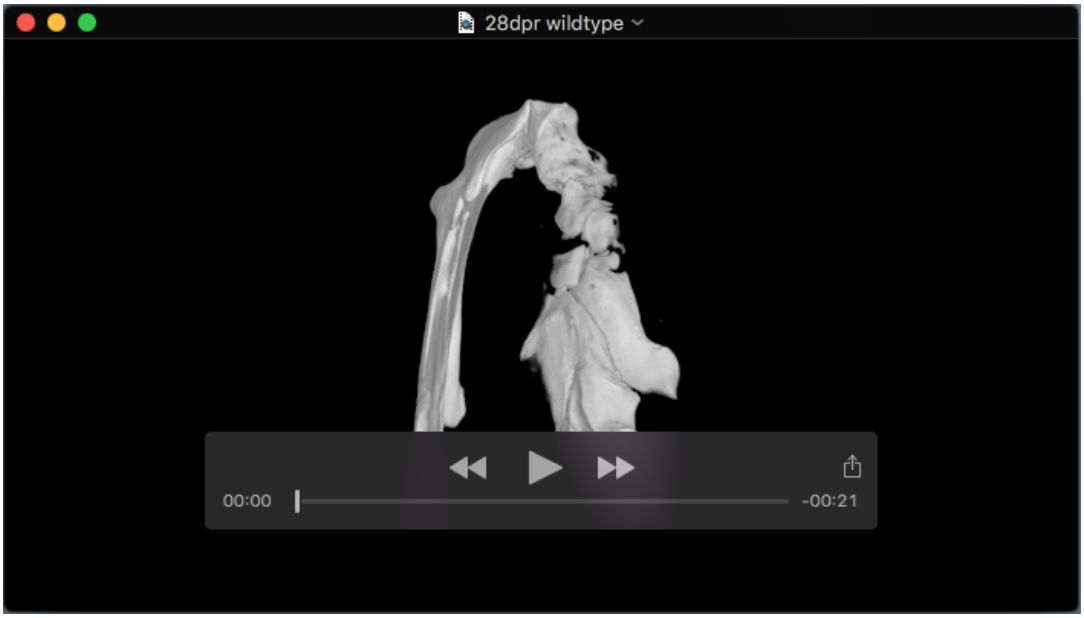

Movie 2. Volume reconstruction of µCT scans of 28 dpr wild-type sibling of an *ihha* mutant. Note the near complete bridging and thickness of the bone.

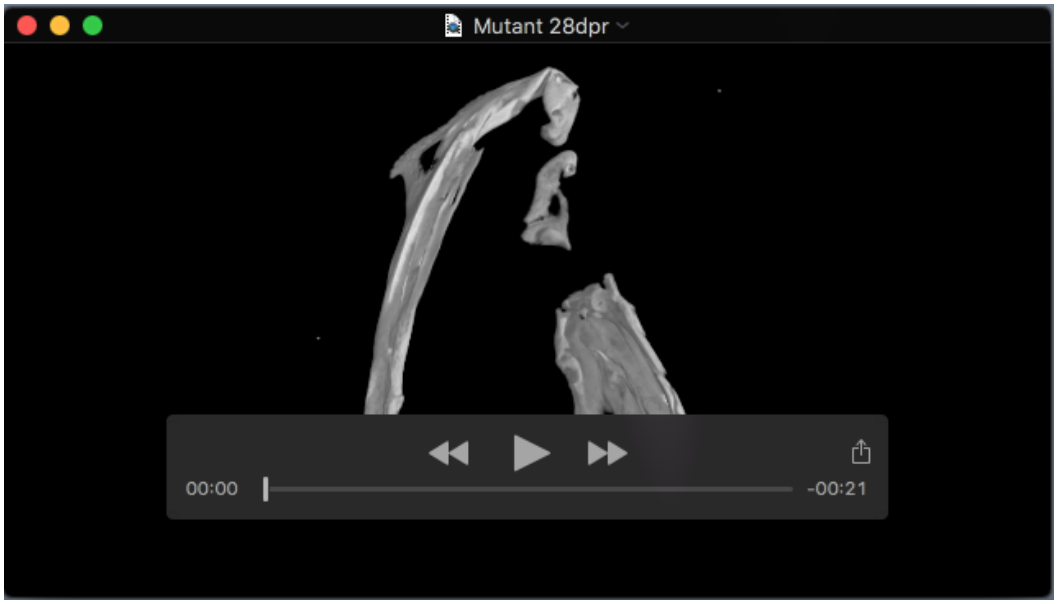

Movie 3. Volume reconstruction of µCT scans of 28 dpr *ihha* mutant shows incomplete bridging and hollow bone.

Table S1. Primers used for riboprobe synthesis.

Gene	Fwd Primer	Rev Primer	Probe Length	
col1a1a	GTATTGTAGGTCTCCCTGGACAAA	TGTTCTTGCAGTGGTATGTAATGTT	1239bp	HindIII, T7
col2a1a	GTAAAGATGGAGAGACTGGACCTTC	ATTCTCTCCTCTGTCTCCCTGTTT	1376bp	NotI, SP6
col10a1	GTCTAAAAGGTGACAGAGGAGTACCT	GTAGACACTGATCAGTAACAAGGAAACA	1421bp	HindIII, T7
spp1	AACGGCCACCTCCTATTCTT	CACTGCCGTCTGTCGTCTAA	1399bp	HindIII, T7
runx2b	GATGTACTTTTCCTGATAACTGGAGTG	CACAGCTATTTCGCTTTATACTGTAGG	1657bp	HindIII, T7
sp7	GTCAATACTTATTTAGACATGACGCATCCTTAC	GCAAGTTTTGAGAAAAACTTTGTATTCACTCTA	1993bp	NotI, SP6
bglap	CTCTGAGCTGACAATATCAACTAAACA	GGTTCTAGAAGGGAATGGGCCCATA	342bp	NotI, SP6
ctgfa	AGAGTCTTTCCAGAGCAGTTGTAAATA	CTCTGAGCTGACAATATCAACTAAACA	1216bp	HindIII, T7
ihha	AACCGCTGAGCAACAGGTTTAAT	GACAAATGGGTTCAAAGGATATGGTATAA	1625bp	SpeI, T7
ihhb	GTTATCTTCACCGTCTTTGACACTC	TGGAAGAGTTCTGATTCTAGCAGTAGT	1657bp	NotI, SP6
gli1	ATATGGAAACTCTCCCCTAAAACACAACTTTAC	GAATTTGCTTTAGTTTGTCGATCTTCAGGTT	2115bp	HindIII, T7
ptc1 (ENSDARG00000055026)	GACTTTGGCTCAAGGAAAGACTAGAGAATA	GTACCATAGAGGCTGAGGCTTAAAAGAG	2428bp	NotI, SP6
ptc2 (ENSDARG00000016404)	GCCCAGTTCCGTTATTTTTCATTCTAC	GTCTCCTGAAGTCTGATAGCTGTCATTG	1857bp	NotI, SP6

Table S2. Experimental numbers.

Figure	Experimental numbers
1	**Regeneration of the lower jawbone in adult zebrafish**
1A,B	Skeletal staining of un-resected animal (n = 9)
	Skeletal staining of 0 dpr animal (n = 4)
	Skeletal staining of 7 dpr animals. 5/9 displayed more than 50% bridging. 3/9 displayed up to 50% bridging and 1/9 did not show any cartilage response. Additionally 5/9 animals showed about 20% deposition of bone at the cut surface
	Skeletal staining of 14 dpr animals. 7/11 animals displayed more than 50% cartilage across the resected region and variable degrees of mineralized matrix. 8/11 animals displayed about 80% mineralization across the lesion,

	and 3/7 animals displayed about 50% mineralization.
	Skeletal staining of 35 dpr animals. 6/7 animals displayed complete bridging of the gap by mineralized matrix. 1/7 animal showed about 80% bridging of mineralized matrix. 5/7 animals had more than 50% bridging of cartilage (intermingled with bone) while 2/7 animals had about 20% cartilage left.
1C	H&E for un-resected animals (n = 5)
	H&E for 10 dpr (n = 5/5 animals showed chondrocytes embedded in regenerating bone edges while extensive cartilage was present within the resected region).
	H&E for 30 dpr (n = 4/4 animals showed increased matrix deposition around chondrocytes in regeneration and the edges of cartilage callus showed transition to bone histology).
	H&E for 60 dpr (n = 3/3 animals showed extensive bone formation and very few cells with chondrocyte morphology entrapped in the bone matrix).
1D	Representative example from 1B for 35dpr and unresected control.
2	**Co-expression of chondrocyte and osteoblast programs in repair cartilage.**
2A	*sox9a* ISH at 6 dpr (n = 3/6 had expression in regenerating cartilage, n = 4/6 in mesenchyme), 8 dpr (n = 6/6 in regenerating cartilage as well as mesenchyme), 10 dpr (n = 5 in regenerating cartilage),
	col2a1a ISH at 6 dpr (n = 5/6 in regenerating cartilage, n = 6/6 in mesenchyme), 8 dpr (n = 7/7 strong expression in regenerating cartilage), 10 dpr (n = 8/8 strong expression in regenerating cartilage).
	col10a1 ISH at 6 dpr (n = 0/6 show expression in regenerating cartilage), 8 dpr (n = 5/5 in regenerating cartilage), 10 dpr (n = 8/8 in regenerating cartilage)
	runx2b ISH at 6 dpr (n = 6/6 in mesenchyme, 2/6 in regenerating cartilage), 8 dpr (n = 4/4 in regenerating cartilage), 10 dpr (n = 5/5 in regenerating cartilage),
	col1a1a ISH at 6 dpr (n = 3/3 show strong expression in injured periosteum, n = 3/3 in mesenchyme surrounding the cut bone, n = 3/3 in regenerating cartilage in salt and pepper manner), 8 dpr (n = 6/6 show strong expression in periosteum, n = 6/6 in mesenchyme spanning the lesion, n = 6/6 strong expression in regenerating cartilage), 10 dpr (n = 4/4 strong expression in regenerating cartilage)
	spp1 ISH at 6 dpr (n = 3/3 very weak expression in periosteum), 8 dpr (n = 3/3 weak expression in periosteum), 10 dpr (n = 3/3 in regenerating cartilage)
2B	*col2a1a/col1a1a* two color ISH at 10 dpr (n = 3/3 show co-expression in cells of the regenerating cartilage)
	col2a1a/runx2b two color ISH at 10 dpr (n = 4/4 show co-expression in cells in the regenerating cartilage)
3	**Mineralization and osteocyte maturation of repair chondrocytes.**
3A	Trichrome staining at 8dpr (n = 4)
3B	*col2a1a*^{BAC}:GFP/Alizarin red at 30 dpr (n = 13/13 animals showed chondrocytes embedded in calcified matrix.
3C	a-GFP/*spp1* on 16 dpr *col2a1a*^{BAC}:GFP (n = 2/2 with expression in cartilage)

3D	a-GFP/*col2a1a* on 30 dpr *col2a1a*^{BAC}:GFP (n = 5/5 with expression in cartilage)
	a-GFP/*bglap* on 30 dpr *col2a1a*^{BAC}:GFP (n = 3/3 with expression in cartilage)
4	**Development of growth plate cartilage in juvenile zebrafish**
4A	Trichrome staining at 14 dpf (n = 2)
4B,C	*col10a*/a-BrdU/a-GFP on sp7:GFP 28 dpf (n = 2)
4C	*sox9a/col1a1a* in ceratohyal at 14 dpf (n = 2)
	col2a1a/col1a1a in ceratohyal at 14 dpf (n = 3)
	col2a1a/spp1 in ceratohyal at 14 dpf (n = 3)
	col2a1a/col1a1a in ceratohyal at 21 dpf (n = 3)
	col2a1a/bglap in ceratohyal at 28 dpf (n=4)
	col2a1a/col10a1 in ceratohyal at 28 dpf (n=2)
4D	Perichondral mineralization of *col2a1a*^{BAC}:GFP (n=3 at each stage)
5	**Mobilization of the periosteal cells in response to jaw resection.**
5A, B	H&E staining of re-sected jawbone in un-resected WT (n = 3) and at 0 dpr (n = 3), 2 dpr (n = 3), 4 dpr (n = 3), and 6 dpr (n = 3)
5C	Anti-BrdU/*col1a1a* in un-resected adult (n = 2), 4 dpr (n = 2)
5D, E	Anti-GFP/anti-mCherry in uninjured RUNX2:GFP;sp7:mCherry adult animals (n = 4/4)
5F	Anti-GFP in runx2:GFP line at 4 dpr (n = 3), and 7dpr (n = 3)
5F	Anti-GFP in sp7:GFP line at 4 dpr (n = 3), and 7dpr (n = 4)
6	**Requirement of ihha in the generation of repair cartilage.**
6A	*ptc2* expression at 6dpr (n=2/2 animals show ptc2 expression in nascent cartilage and pre cartilaginous mesenchyme).
	sox9a/ptc1 at 8dpr (n = 2/2 animals show *ptc1* co-expressing with *sox9a*+ cells.
	ihha colorimetric ISH at 10 dpr (n = 6/6 in regenerating cartilage)
	gli1 colorimetric ISH at 10 dpr (n = 6/6 in regenerating cartilage)
6B	Alcian blue-alizarin red labeling of cartilage and bone at 14 dpr in *ihha-/-* (n = 3) & WT siblings (n = 4)
	Alcian blue-alizarin red labeling of cartilage and bone at 28 dpr in *ihha-/-* (n =9) & WT siblings (n = 10).
6C	µCT analysis of same animals depicted in alcian-alizarin images in 6B
6D	Quantification of BrdU+ nuclei in *ihha-/-* vs WT (2 sections from 2 animals each).
6E	BrdU incorporation in 4 dpr WT (n = 2) and *ihha-/-* (n = 2) animals.
6F	BrdU+ nuclei in Col2:GFP+ cells n=3/3 wildtype showed extensive cartilage while n=3/3 *ihha-/-* mutants showed severe reduction of chondrocytes
6G	Quantification of BrdU+ nuclei/100 chondrocytes. n = 3/3 animals show no significant difference in chondrocyte proliferation in *ihha-/-* vs wild types.
6H	Anti-Sox9a/anti-GFP staining on *ihha-/-*, *col2a1a*^{BAC}:GFP (n = 2/3 animals showed small nodules of cartilage with very few chondrocytes expressing Sox9a/GFP while 1/3 did not show any cartilage); and WT siblings (n = 3/3 animals showed large areas of Sox9a/GFP+ chondrocytes)

S1A	Un-resected adult zebrafish jaw (n = 4)
S1B	Bone fragment taken out after resection (n = 6)
S2A	*sp7* expression at 6 dpr (n = 3/3 weak expression in periosteum)
S2B	*sp7* expression at 10 dpr (n = 3/3 in regenerating cartilage)
S2C	*ctgfa* expression at 14 dpr (n = 3/3 animals showed expression in subsets of chondrocytes)
S2D	*ihhb* expression in 14 dpr animals. (n = 2/2 animals showed very weak expression in regenerating cartilage versus strong expression in the growth plates of the ceratohyal
S2E	Triple fluoresecnt ISH for *col1a1a, col2a1a* and *col10a1* at 14 dpr (n = 2/2 animals showed co-expression of all three genes in regenerating chondrocytes)
S2F	*col1a1a* ISH/ anti-GFP in Col2:GFP line n=5/5 animals show well segregated *col1a1a* expression in periosteum and GFP expression in Meckel's cartilage.
S2G	Anti-sp7/anti-GFP immunofluorescence in osteocalcin:GFP line, n = 4/4 animals show cells co-expressing as well as individually expressing these markers.
S2H	*col1a1a* expressing cells are a subset of sp7:GFP+ cells (n = 3/3)
S3A	anti-Sox9a immunohistochemistry (n = 8/8 animals showed Sox9a immunoreactivity in regenerating cartilage)
S3B	anti-Sp7 immunohistochemistry (n = 3/3 animals showed Sp7 immunoreactivity in a minority of regenerating chondrocytes)
S3C	anti-Col1a1a immunohistochemistry (n = 4/4 animals showed Col1a1a immunoreactivity in regenerating cartilage)
S3D	anti-Col2a1 immunohistochemistry (n = 3/3 animals showed Col2a1 immunoreactivity in regenerating cartilage, but more so at edges of cartilage).
S4A	H&E staining of 30 dpr *col2a1a*^{BAC}:GFP animals (n = 3/3 animals showed cells embedded in newly formed bone at the edge of regenerating cartilage)
S4B, C	anti-GFP staining on adjacent sections from Fig S4A (n = 3/3 animals showed GFP+ cells embedded in bone at the edge of the regenerating cartilage)
S5A	*col2a1a* mRNA/anti-GFP in 30 dpf *col2a1a*^{BAC}:GFP fish (n = 3/3 animals showed that *col2a1a* mRNA is restricted to growth plates in ceratohyal, while GFP protein persists in the entire ceratohyal).
S5B	*gfp* mRNA/anti-GFP in 30 dpf *col2a1a*^{BAC}:GFP fish (n= 3/3 animals showed *gfp* mRNA restricted to growth plates and GFP protein throughout the ceratohyal).